Adsorption of Blood Proteins onto Polysaccharide Surfaces

Xinyi Tan

Thesis submitted to the faculty of the
Virginia Polytechnic Institute and State University
in partial fulfillment of the requirements for the degree of

Master of Science
in
Macromolecular Science and Engineering

Maren Roman, Chair
Alan R. Esker
Kevin J. Edgar

September 30, 2015
Blacksburg, VA

Keywords: albumin, fibrinogen, cellulose acetate, cellulose, thin films, adsorption

Adsorption of Blood Proteins onto Polysaccharide Surfaces

Xinyi Tan

Abstract

In this study, surface plasmon resonance (SPR) and quartz crystal microbalance with dissipation monitoring (QCM-D) were combined to investigate the adsorption behavior of two platelet adhesion-related blood proteins, human serum albumin (HSA) and human serum fibrinogen (HSF), on two polysaccharide materials used for hemodialysis membrane applications: regenerated cellulose and cellulose acetate. The study aims to provide insight into the design of novel hemocompatible polysaccharide materials. Information such as real-time adsorption curves, adsorbed amounts, and water contents of the protein layers were obtained and analyzed. The results suggested 1) monolayer adsorption of HSA on both cellulose and cellulose acetate, possibly with different HSA conformations; 2) a multilayer of HSF or some degree of end-on adsorption on both surfaces. The study of HSA adsorption onto cellulose acetate surfaces with different degrees of substitution indicated that the change in content of acetyl groups may not be the main factor governing the adsorbed HSA amount but may affect the conformation of adsorbed HSA molecules.

Acknowledgements

First of all, I would like to express my gratitude to my advisor, Prof. Maren Roman, for her support and guidance during my studies and research at Virginia Tech. Without her patience, encouragement, and suggestions, I would not have accomplished this work. I greatly appreciate the tremendous time and effort she invested for helping and motivating me to proceed with this project. I also would like to thank my committee members: Prof. Alan R. Esker and Prof. Kevin J. Edgar for their insightful comments and advice. Prof. Esker is always open for discussions when I need help. And Prof. Edgar always provided many helpful suggestions during my seminar presentations.

I'm truly grateful to Prof. Judy S. Riffle and all other administrative faculty and staff of the Macromolecules and Interfaces institute and the Department of Sustainable Biomaterials for their assistance during my studies in the MACR program.

I would like to thank my colleague Feng Jiang for his training in using the QCM-D instrument, Jung Ki Hong for his training in using the AFM, and Jianzhao Liu in Dr. Esker's group for his help with the SPR measurements. I also want to thank many other colleagues: Dr. Hezhong Wang, Shuping Dong, and Chen Qian in Dr. Roman's group, Dr. Chao Wang, Dr. Xiao Zhang, and Sumin Shen in Dr. Esker's group, Dr. Daiqiang Xu, Dr. Siddhesh Pawar, Dr. Haoyu Liu, Xueyan Zheng, Ruoran Zhang, and Yifan Dong in Dr. Edgar's group, and Wei Zhang in Dr. Renneckar's group for their assistance, discussions, and encouragement during my research. Special thanks to Yi Yang, who is a great friend, for her companionship and encouragement throughout my studies.

Finally, I want to express my deepest gratitude and appreciation to my parents for their unconditional love and support through these years.

Table of Contents

List of Figures

Chapter 2

Chapter 3

Chapter 4

Appendix A

List of Tables

Chapter 2

Chapter 3

Chapter 4

Chapter 1 Overview

Nowadays, polysaccharides – a class of sustainable materials – are widely used for many biomedical applications. For example, cellulose and cellulose derivatives are being commercially used as membrane materials for hemodialysis treatment. In the hemodialysis process, the materials that are involved come in contact with blood. Being one of the first events during blood–material contact, the adsorption of proteins onto the material's surface has a great effect on the compatibility of the material with blood and related surface interactions. There are two blood proteins that have been found to be closely related to platelet adhesion. They are human serum albumin (HSA) and human serum fibrinogen (HSF). This research studies the adsorption behavior of HSA and HSF on different polysaccharide surfaces. The main aspects of interest include the time dependence of adsorption, irreversibly adsorbed amount, and water content of the protein layers. The two major techniques used are quartz crystal microgravimetry with dissipation monitoring (QCMD) and surface plasmon resonance (SPR).

This thesis consists of five chapters:

Chapter 1 gives a general overview of the thesis content.

Chapter 2 provides an overall introduction and literature review of background information related to the research. It begins with the concept of biomaterial hemocompatibility and the three main pathways for blood–material interactions. Next, the major categories of membranes used for hemodialysis and their interactions with blood are reviewed. Finally, the chapter reviews some fundamental properties of proteins relevant to protein adsorption and provides a detailed discussion of HSA and HSF.

Chapter 3 and Chapter 4 describe the QCMD and SPR adsorption experiments with HSA and HSF on polysaccharide surfaces. Each chapter consists of five parts: abstract, introduction, experimental section, results and discussion, and conclusions. While Chapter 3 focuses on the different adsorption behavior of the two blood proteins on two polysaccharide surfaces: regenerated cellulose and cellulose acetate (CA), Chapter 4 focuses on how the density of acetyl groups on CA affects the adsorption behavior of HSA.

Chapter 5 gives the overall conclusions of this thesis and some suggestions for the future works.

Chapter 2 Literature review

2.1 Hemocompatibility

Polysaccharide-based materials are being widely used in medicine and many new applications are under investigation. Examples include oxidized cellulose, chitin, and chitosan used as topical hemostatic agents to control bleeding, regenerated cellulose and cellulose derivatives used as hemodialysis membranes, and bacterial cellulose sheets and tubes used as temporary covers for burn wounds and artificial blood vessels [1-5]. In these applications, the materials come in contact with blood. Consequently, hemocompatibility is an important factor to consider in their overall performance.

The term biocompatibility is commonly defined as "the ability of a material to perform with an appropriate host response in a specific application." Hemocompatibility is biocompatibility with blood. For a blood-contacting device, it is mainly related to thrombotic responses induced by materials [6]. The blood–material interactions begin with protein adsorption onto the material surfaces, which then triggers a complicated and interlinked series of events. The three main adverse responses are (i) inflammation and white cell depletion caused by leukocyte interactions, (ii) blood coagulation via the intrinsic pathway, and (iii) platelet adhesion and activation [6, 7]. A schematic is shown in Figure 2.1. These thrombotic responses are not independent. For example, while adherent platelets provide a catalyst in coagulation, the thrombin generated in the coagulation process can activate platelet adhesion [7]. Both platelet-mediated reactions and blood coagulation contribute to the surface induced thrombus consisting of fibrin, platelets, and red blood cells [7, 8].

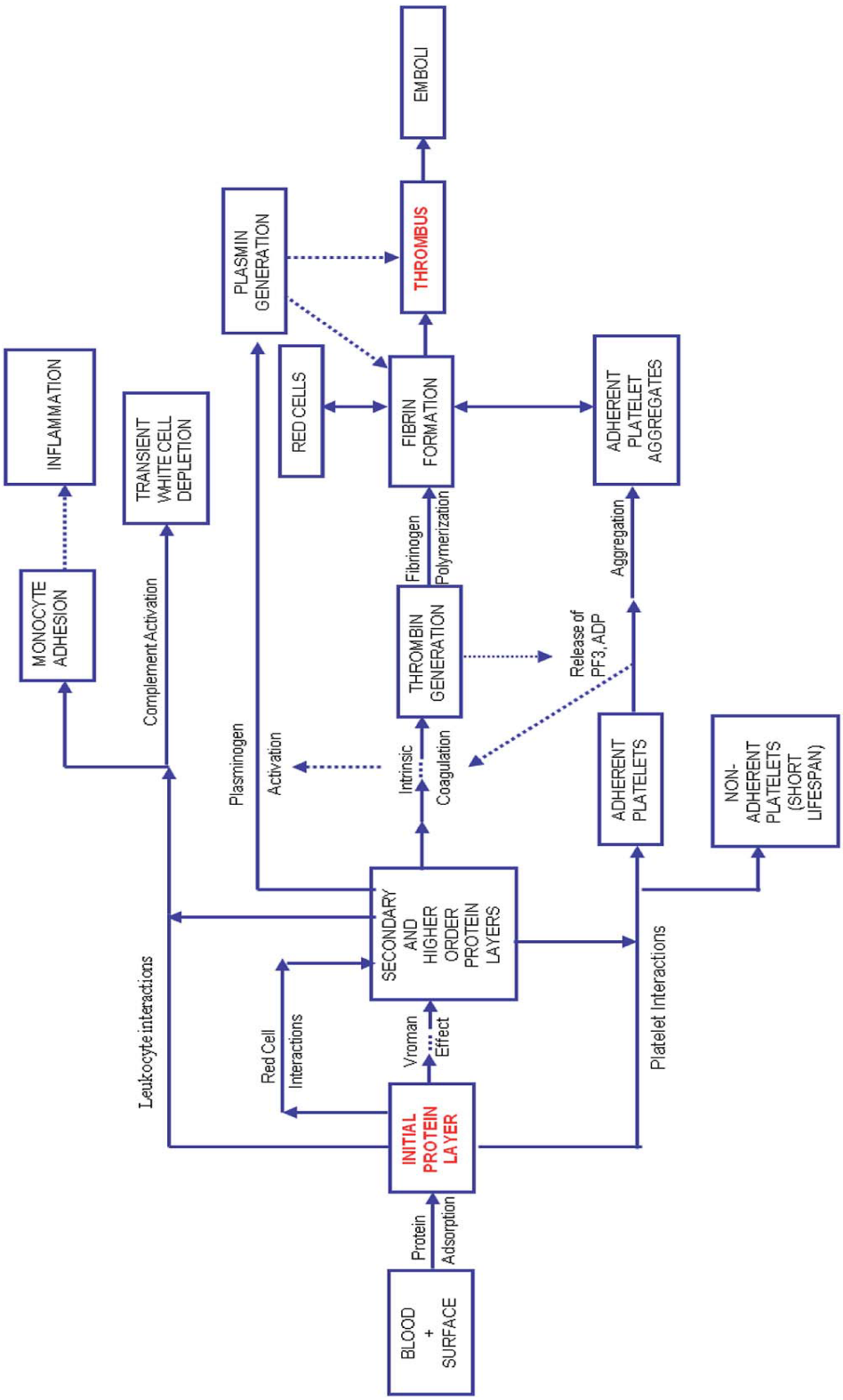

Figure 2.1 Interaction between blood and material surfaces [7] (Reprinted from ref 7; Fair use; Copyright Royal Society of Chemistry 2015)

2.1.1 Blood coagulation

Blood coagulation is a fibrin formation process. The coagulation cascade of fibrin formation can be divided into two pathways: the contact activation pathway and the tissue factor pathway. The contact activation pathway is also called the intrinsic pathway, because the blood itself already contains all necessary proteins to cause blood coagulation [9]. The tissue factor pathway is also called the extrinsic pathway, because this path needs a substance from the cut tissue of a wound [9]. The two pathways differ but merge at the step of FIIa (activated form of FII) formation. A schematic is shown in Figure 2.2.

For blood contacting materials, the intrinsic pathway has more clinical importance. The cascade begins with surface-contact activation of the blood zymogen FXII (Hageman factor). The activation complex including FXIIa, FXI, the prekallikrein and high-molecular-weight kininogen leads to thrombin formation [8, 10, 11]. And thrombin finally cleaves fibrinogen into fibrin monomers, which then polymerize and cross-link to form a fibrous mesh.

FXII activation (also called autoactivation) is vital for the coagulation process, and was found to have an obvious specificity for anionic or hydrophilic surfaces. It is generally believed that the negative charges on hydrophilic surfaces may cause conformational changes of FXII *via* its positively charged amino acids in the heavy chain, which leads to autoactivation [10, 12]. Another theory proposes that the degree of contact activation is more related to the presence of proteins and unrelated to the coagulation cascade in the fluid phase, known as “adsorption-dilute” effect [8, 13, 14]. The competing adsorption between high concentration blood proteins (such as albumin, fibrinogen, or IgG) and FXII greatly reduces the contact of FXII with hydrophobic

surfaces, while an enhancement of autoactivation of FXII may occur on hydrophilic surfaces at the same time [8, 13, 14]. The proteins involved in blood coagulation are listed in Table 2.1.

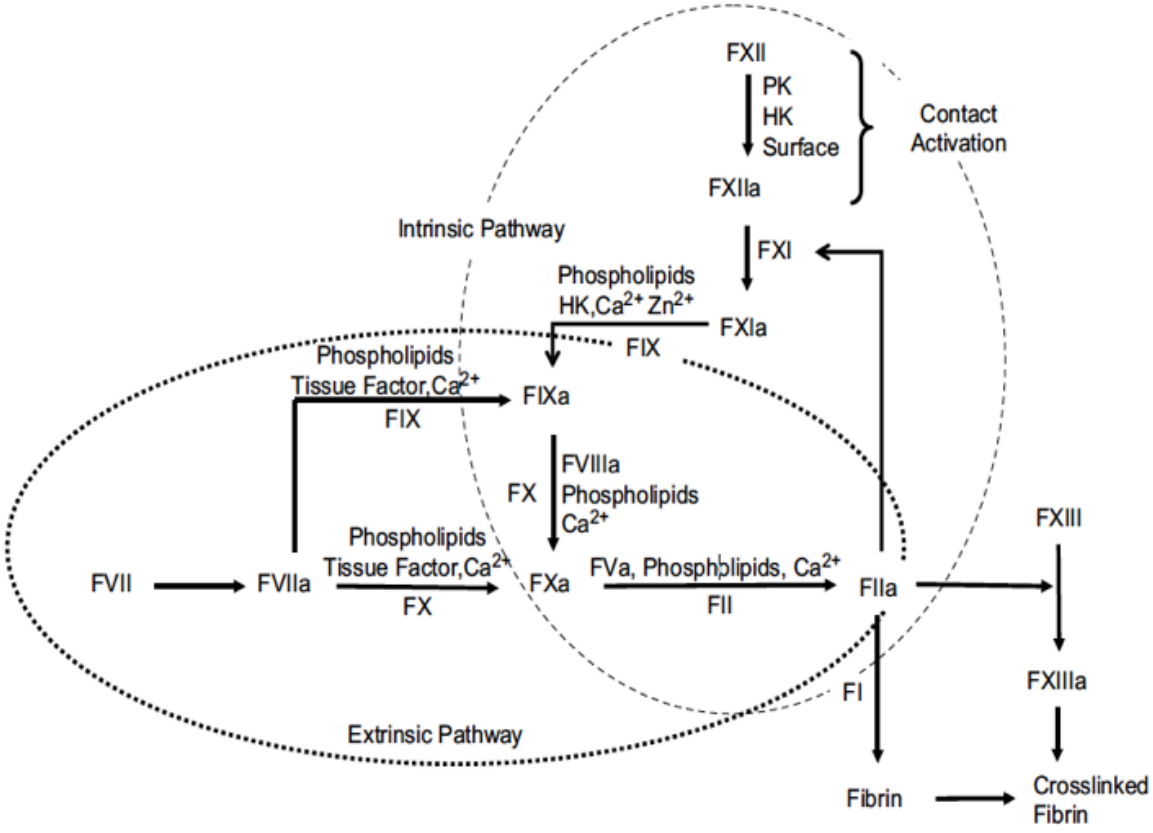

Figure 2.2 Intrinsic and extrinsic blood coagulation pathways [8] (Reprinted from ref 8; Fair use; Copyright 2008 Elsevier Ltd.)

Table 2.1 Blood coagulation factors [8] (Adapted from ref 8; Fair use; Copyright 2008 Elsevier Ltd.)

Blood coagulation factor	Common names
FI	Fibrinogen
FII	Prothrombin
FIII	Tissue factor/thromboplastin
FIV	Divalent calcium ion
FV	Proaccelerin (labile factor)
FVI	N/A
FVII	Proconvertin (stable factor)
FVIII	Antihemophilic factor
FIX	Christmas factor
FX	Stuart prower factor
FXI	Plasma thromboplastin antecedent
FXII	Hageman factor
FXIII	Fibrin stabilizing factor
Plasma prekallikrein	Fletcher factor
High molecular weight kininogen	Fitzgerald, Williams or Flaujeac factor
Plasminogen	N/A

2.1.2 Platelet adhesion, activation, and aggregation

Platelets are part of a thrombus. They play a main role in forming a plug to preserve the integrity of the vascular wall [6]. Platelets do not interact with the inner surface of normal blood vessels but adhere promptly to exposed extracellular matrix substrates or where endothelial cells are altered [15]. They can adhere to any thrombogenic surface, such as endothelium, subendothelium, or artificial surfaces, and undergo an activation process [6]. The activation causes a change in the surface membranes of the platelets and release of chemicals (platelet factor 4, adenosine diphosphate, and serotonin), which induce the activation of other non-adherent platelets and cohesion with already adherent platelets [7, 16]. This process is called platelet

aggregation. Both adhesion and aggregation are mediated by the same adhesive ligand and receptor pairs [15].

Platelet adhesion can be initiated by extracellular matrix components (collagen, von Willebrand factor, fibronectin, laminin, fibulin, and thrombospondin), plasma proteins (thrombin and fibrinogen), and molecules derived from inflammatory cells [15, 17-20]. A list of platelet receptors and their specific agonists/ligands is presented in Table 2.2. GPIb and GPIIb/IIIa have the highest density on platelets among the different adhesion receptors [6]. Platelet activation can happen during contact with biomaterials and is procoagulant in nature [6]. It was found to be related to the interaction between receptors and specific amino acid sequences of adsorbed proteins. The receptor on the activated platelet surfaces undergoes a conformational change and binds to RGD sequences of adsorbed proteins [7].

Table 2.2 Platelet adhesion receptors [6] (Adapted from ref 6; Fair use; Copyright 2004 Elsevier Ltd.)

Receptor	Ligand/agonist
GPIa/IIa or VLA-2	Collagen
GPIb/IX or GPIb	VWF, thrombin
GPIc/IIa or VLA-5	Fibronectin
GPIc'/IIa or VLA-6	Laminin
GPIIb/IIIa	Collagen, fibrinogen, fibronectin, vitronectin, VWF
GPIV or GPIIIb	Collagen, thrombospondin
GPVI	Collagen
Vitronectin receptor	Vitronectin, thrombospondin
PECAM-1	Heparin
Fcγ-RII	Immune complexes
ICAM-2	LFA-1
P-selectin	Sialyl-Le^x
Leukosialin, sialophorin	ICAM-1

GP: glycoprotein; VWF: Von Willebrand factor; VLA: very late antigen

2.2 Hemodialysis membrane

Hemodialysis is a medical treatment method for patients with renal failure used to remove waste products, such as creatinine and urea, from the body but allow the transport of water. The hemodialysis membrane is usually semipermeable with different pore sizes and its performance is largely determined by its solute removal efficiency and selectivity. Besides these parameters, the biocompatibility of the membrane is of important consideration.

2.2.1 Membrane categories

Cellulosic membranes have been used since the time of the first hemodialysis treatment. The first membrane material, Cuprophan®, prepared by dissolving cotton-derived cellulose in an ammonia solution of cupric oxide, is still in use today [21, 22]. But this material was found to cause both complement and platelet activation [23]. Complement activation is believed to occur via the alternative pathway through the covalent binding of complement activation product C3b to surface hydroxyl groups of cellulose [24, 25].

Modified cellulosic membranes were designed to reduce complement activation by substitution of the hydroxyl groups (Figure 2.3). Commonly used modified cellulosic membranes have quite different design strategies. Cellulose acetate membranes, composed of either cellulose diacetate (Diaphan®) or cellulose triacetate [26], cause less complement activation, which can be explained by a great reduction in the binding of C3b [27]. For Hemophan®, however, 5% of the hydroxyl groups are modified with tertiary amine groups. One possible explanation for the increased hemocompatibility of

Hemophan® is that the bulky groups sterically shield the remaining hydroxyl groups and, thus, decrease the interaction of the material with complement activation products [4, 28]. Synthetically modified cellulose (SMC), a low benzyl substituted cellulose, is believed to have a similar mechanism for increased hemocompatibility [4, 29]. Another mechanism that has been proposed is the adsorption of complement factor D and H, which act as regulators in the complement cascade [4].

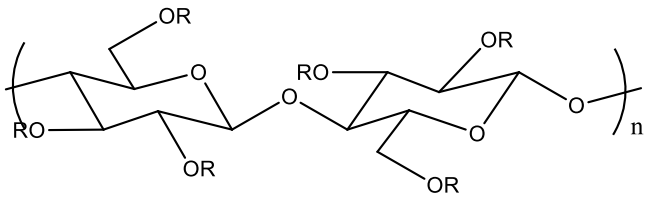

Cellulose Acetate: R = –H or $–OC(O)CH_3$

Hemophan®: R = –H or $–OCH_2CH_2N^+(CH_2\,CH_3)_2$

Synthetically modified cellulose: R = –H or $–OCH_2OC_6H_6$

Figure 2.3 Chemical structure comparison of modified cellulosic membranes

The second mechanism is thought to be more relevant to synthetic membranes, which can adsorb complement factors unspecifically. Examples of synthetic membranes include polysulfone, polymethylmethacrylate (PMMA), and polyamide [24]. Most synthetic polymers are too hydrophobic and need to achieve a hydrophobic-hydrophilic balance for use, because highly hydrophobic materials activate platelets through adsorption of blood proteins [4].

2.2.2 Platelet interaction with membranes

Platelet adhesion is another important aspect of compatibility of hemodialysis membranes. Both platelet–platelet and platelet–leukocyte aggregation have been detected

in the blood eluting from the dialyzer, which may cause a decrease in platelet count number [30]. A decrease in platelet count is typically observed at the beginning of hemodialysis; but platelet count may return to its initial value at the end of the procedure [30]. Reuse of hemodialysis membranes decreases platelet activation [30].

Many studies have been done on the effect of hemodialysis membranes on platelet count and function. A good review of the topic was done by Daugirdas and Bernardo [30]. Generally, cellulose acetate and other synthetic membranes, such as polysulfone, polyacrylonitrile, polymethylmethacrylate, cause a similar drop in platelet count, which is lower than that caused by Cuprophan membranes [26, 31-35]. Studies of platelet activation and degranulation during dialysis with different surface markers have also shown that synthetic membranes generally cause less platelet activation than cellulosic membranes [30, 36]. The exact causes and clinical consequence of platelet interactions remain unknown.

2.3 Protein adsorption and platelet adhesion

Protein adsorption is the initial event during material–blood contact and is greatly influenced by the surface properties of the material, including hydrophobic-hydrophilic balance and functional groups [10]. The hemocompatibility of biomaterials is greatly dependent on the interaction between blood proteins and material surfaces. Platelet interactions are mediated by platelet surface receptors that bind to adsorbed proteins. Thus, the study of protein adsorption behavior is important in the design of novel biocompatible materials.

2.3.1 Protein structure

Proteins are constructed from 20 amino acids and have a unique structure with 4 levels (Figure 2.4). The primary structure describes the amino acid sequence of the peptide backbone [37-39]. The amino acids are linked via peptide bonds; and two of three bonds are flexible to rotate to form different spatial arrangements [37-39]. The secondary structure describes repetitive structure units such as α-helix and β-sheet (Figure 2.5). Hydrogen bonding exists between amide and carbonyl groups of peptide backbones and contributes to structural stability. The tertiary structure describes the three-dimensional folding arrangement of polypeptides, which is greatly determined by the primary structure. The quaternary structure describes the combination of tertiary structures [37-39].

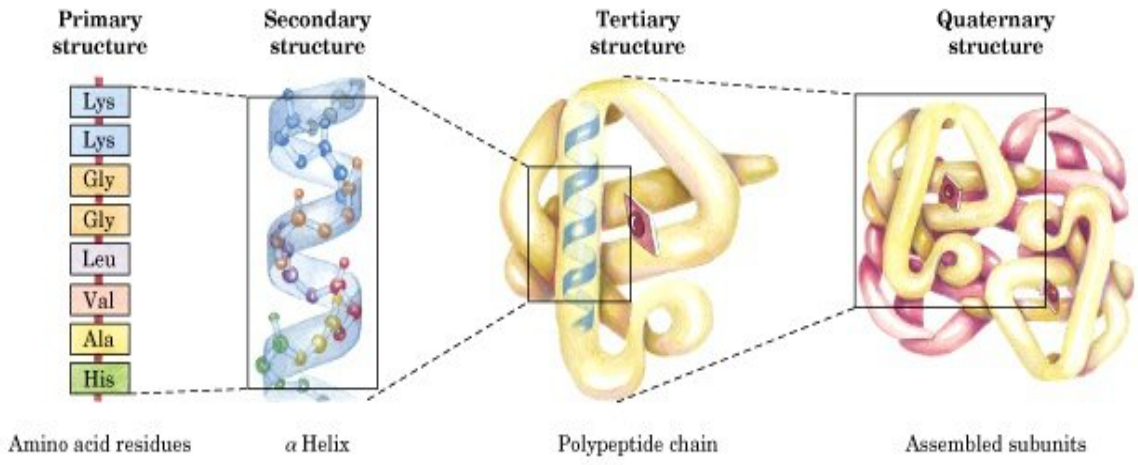

Figure 2.4 The four levels of protein structure [40] (Reprinted from ref 40; Fair use; Copyright Worth Publishers)

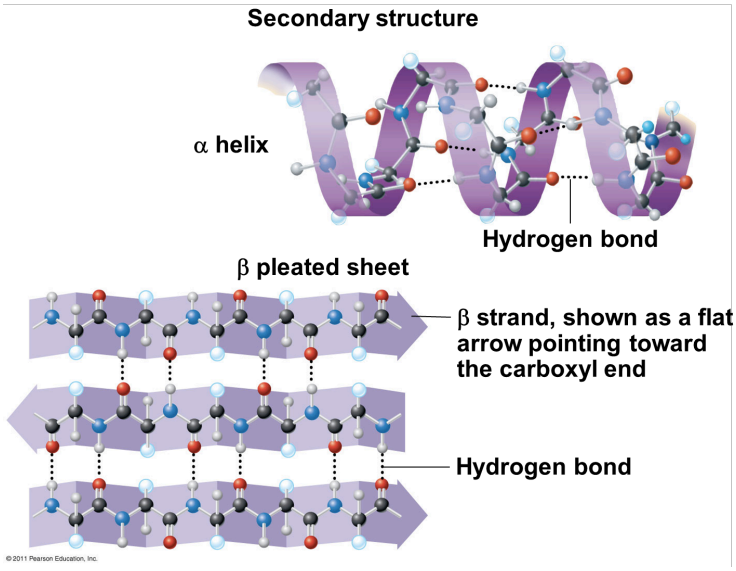

Figure 2.5 Secondary structure of proteins (α-helix and β-sheet) [41] (Reprinted from ref 41; Fair use)

The properly folded and reactive conformation is called the native state of the protein. The conformation of a protein is very sensitive to the surrounding environment such as temperature, pH, ionic strength, and surface energy. Protein denaturation happens if the quaternary, tertiary, or secondary structure changes. Proteins can return to the native state from a limited range of conformations. Outside of this range, denaturation is irreversible; and proteins form misfolded structures, losing their biological function, and may aggregate. Proteins can be divided into two groups on the basis of their internal stability: soft proteins (e.g. albumin, immunoglobulin), with low conformational stability, and hard proteins (e.g. fibrinogen), with a higher stability [37-39, 42-44].

2.3.2 Protein adsorption process

Protein adsorption is a complicated process, resulting from the combination of the interactions with the sorbent surface, among proteins, with the solvent, and with other

solutes. These interactions include hydrophobic interactions, electrostatic forces, and hydrogen boding. When $\Delta_{ads}G = \Delta_{ads}H - T\Delta_{ads}S < 0$, adsorption is spontaneous. G, H, S and T are the Gibbs free energy, enthalpy, entropy, and absolute temperature, respectively. Δ_{ads} represents the change of the thermodynamic function during adsorption [37-39, 42-44].

Hydrophobic dehydration is a common driving force for protein adsorption. When proteins and the adsorbent surface get dehydrated, the entropy of the water molecules increases, which results in a decrease of the Gibbs free energy of the system. Generally, an interaction with a hydrophobic surface is more favorable with a larger entropy gain [37-39, 42-44]. Also, proteins adsorb more strongly to the nonpolar substrates.

Electrostatic interactions come into play when surfaces are charged because proteins may also be charged, depending upon solution pH. Charged surfaces are surrounded by counter ions, which are arranged above these surfaces in electrical double layers. When a protein approaches a charged surface, their electrical double layers overlap. Electrostatic interactions result in a redistribution of charges on both the surface and the protein. Electrostatic repulsion may prevent protein adsorption [37-39, 42-44].

A conformational change can also contribute to the adsorption of proteins. Proteins are highly ordered structures with low conformational entropy. The unfolding of proteins on surfaces can result in an increase in entropy. Thus, the conformational stability of proteins is an important factor to consider. Usually, soft proteins adsorb onto a wide variety of hydrophilic and hydrophobic surfaces because the entropy gain associated with the conformational change can overcome unfavorable conditions, such as electrostatic repulsion. Conversely, hard proteins usually adsorb more readily onto

hydrophobic surfaces [37-39, 42-44].

Whether protein adsorption is reversible or irreversible depends upon both protein properties (hard or soft) and surface properties (hydrophobic or hydrophilic) [42]. Protein desorption may happen when the environment, such as ionic strength or pH, changes [42]. Hard proteins easily desorb from hydrophilic surfaces because of small conformational changes; while the adsorption of soft proteins is often irreversible [42].

2.3.3 Adsorption of blood proteins

The adsorption of blood proteins onto biomaterials follows some basic rules. They are: 1) The adsorption of proteins essentially follows a monolayer model; 2) The composition of the adsorbed protein layer is determined by both affinity and concentration of plasma proteins; 3) The selective adsorption of proteins is greatly dependent upon the surface properties of materials; and 4) The influence of adsorbed proteins on platelet adhesion depends not only upon their amount, but also on their orientation and conformation [45].

The Vroman effect describes the sequential adsorption of blood proteins onto surfaces [46, 47]. The smaller and typically more concentrated blood proteins adsorb onto the surface first and are then replaced with proteins of higher molecular weight and typically higher surface affinity. This phenomenon is closely related to blood coagulation and platelet adhesion [48, 49]. A classic example of the Vroman effect is the displacement of adsorbed fibrinogen by high-molecular-weight kininogen, related to the intrinsic coagulation pathway [7]. Yet, the mechanism of the Vroman effect is not well understood. Other models for protein displacement such as the adsorption/desorption

model or exchange *via* complex formation have been proposed, but none of these models can fully explain the phenomenon [50].

2.3.4 Albumin and fibrinogen

As mentioned above, platelet adhesion can be initiated by binding to adsorbed blood proteins, such as fibrinogen, collagen, and Von Willebrand factor. These proteins are regarded as detrimental to hemocompatibility. However, not all proteins are undesired. It has long been known that the adsorption of albumin reduces platelet adhesion because albumin lacks the specific amino acid sequences for platelet receptor binding [51]. Albumin and fibrinogen are the two most common proteins in human blood and are therefore of great interest.

Albumin is the most abundant protein in human plasma with a normal concentration of 35–50 g/L [52]. It is a single chain, heart-shaped molecule (Figure 2.6) with a molar mass of 67 kDa and has an isoelectric point of 4.7 [52]. The 3D structure of albumin is characterized by a high content of α-helices and a low content of β-sheets [52]. The main role of human serum albumin (HSA) is to maintain the osmotic pressure in blood and to transport hormones, fatty acids, nitric oxide, and other molecules with low solubility [52].

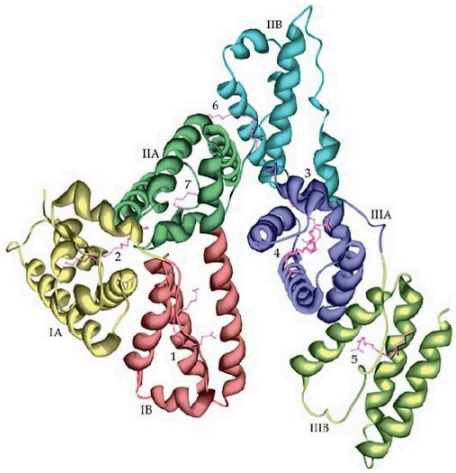

Figure 2.6 Human serum albumin [52] (Reprinted from ref 52; Fair use; Copyright 2008 John Wiley & Sons, Ltd.)

Fibrinogen is the third most abundant protein in human plasma with a normal concentration range of 1.5–4.0 g/L [52]. It is a rod-shaped glycoprotein (Figure 2.7) with a molar mass of about 340 kDa and an isoelectric point of about 5.5 [52]. Structurally, fibrinogen is a dimer of three non-identical chains: Aα-, Bβ-, and γ [52]. Fibrinogen plays an important role in the blood coagulation process, in which it is converted into fibrin by thrombin [52].

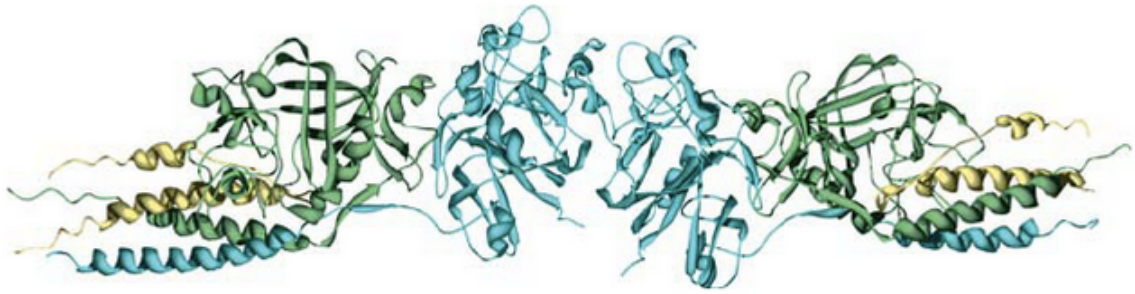

Figure 2.7 Human serum fibrinogen [52] (Reprinted from ref 52; Fair use; Copyright 2008 John Wiley & Sons, Ltd.)

The adsorption behavior of these two proteins has been studied extensively for their significance in surface-induced blood coagulation. Techniques such as surface plasmon resonance, quartz crystal microbalance with dissipation monitoring, circular dichroism, atomic force microscopy, ellipsometry, and Fourier-transform infrared spectroscopy have been used to determine the adsorption behavior and conformational changes [53-58].

Hylton *et al.* found that albumin was not always non-adhesive to platelets. When the conformational change exceeds a critical degree, the platelets can adhere to adsorbed albumin just as to adsorbed fibrinogen [59]. The authors suggested that there is a linear relationship between platelet adhesion and the degree of adsorption-induced protein conformational change [59].

Following this study, Sivaranman *et al.* conducted more detailed studies of the effect of conformational change of adsorbed albumin and fibrinogen on platelet adhesion [60-62]. The authors found some differences in the platelet adhesion inducing mechanism for albumin and fibrinogen [60]. Even when no obvious unfolding of adsorbed fibrinogen was detected, platelet adhesion occurred and increased greatly with increasing degree of unfolding. For albumin, however, platelet adhesion occurred only if the degree of unfolding exceeded a critical degree, that is, 34% loss in α-helix structure [62]. The induced platelet adhesion was believed to be related to the interactions between specific platelet receptors with an RGD sequence (Arg-Gly-Asp) and R residues (arginine) of adsorbed albumin [62]. It was proposed that these residues may not be recognized in the native state of albumin, but structured in a manner and exposed to platelet receptors after

some extent of conformational change [62]. It should be mentioned that albumin undergoes a high degree of unfolding only if its concentration is below 10 g/L, which is lower than its normal level of 40 g/L. Thus, albumin has a minor degree of unfolding at normal concentrations.

2.4 References

[1] PALM, M. D.; ALTMAN, J. S. Topical Hemostatic Agents: A Review. Dermatologic Surgery 2008, 34, 431-445.

[2] Fischer, T. H.; Connolly, R.; Thatte, H. S.; Schwaitzberg, S. S. Comparison of structural and hemostatic properties of the poly-N-acetyl glucosamine Syvek Patch with products containing chitosan. Microscopy Research and Technique 2004, 63, 168-174.

[3] Czaja, W. K.; Young, D. J.; Kawecki, M.; Brown, R. M. The Future Prospects of Microbial Cellulose in Biomedical Applications. Biomacromolecules 2007, 8, 1-12.

[4] Clark, W. R.; Hamburger, R. J.; Lysaght, M. J. Effect of membrane composition and structure on solute removal and biocompatibility in hemodialysis. Kidney Int 1999, 56, 2005-2015.

[5] Achneck, H. E.; Sileshi, B.; Jamiolkowski, R. M.; Albala, D. M.; Shapiro, M. L.; Lawson, J. H. A Comprehensive Review of Topical Hemostatic Agents: Efficacy and Recommendations for Use. Annals of Surgery 2010, 251.

[6] Gorbet, M. B.; Sefton, M. V. Biomaterial-associated thrombosis: roles of coagulation factors, complement, platelets and leukocytes. Biomaterials 2004, 25, 5681-5703.

[7] Liu, X.; Yuan, L.; Li, D.; Tang, Z.; Wang, Y.; Chen, G.; Chen, H.; Brash, J. L. Blood compatible materials: state of the art. Journal of Materials Chemistry B 2014, 2, 5718-5738.

[8] Vogler, E. A.; Siedlecki, C. A. Contact activation of blood-plasma coagulation. Biomaterials 2009, 30, 1857-1869.

[9] Vroman, L. When Blood Is Touched. Materials 2009, 2, 1547-1557.

[10] Sperling, C.; Fischer, M.; Maitz, M. F.; Werner, C. Blood coagulation on biomaterials requires the combination of distinct activation processes. Biomaterials 2009, 30, 4447-4456.

[11] Roberts, H. R. Oscar ratnoff: his contributions to the golden era of coagulation research. British Journal of Haematology 2003, 122, 180-192.

[12] Colman, R. W.; Schmaier, A. H. Contact System: A Vascular Biology Modulator With Anticoagulant, Profibrinolytic, Antiadhesive, and Proinflammatory Attributes. Blood 1997, 90, 3819-3843.

[13] Zhuo, R.; Siedlecki, C. A.; Vogler, E. A. Competitive-protein adsorption in contact activation of blood factor XII. Biomaterials 2007, 28, 4355-4369.

[14] Zhuo, R.; Siedlecki, C. A.; Vogler, E. A. Autoactivation of blood factor XII at hydrophilic and hydrophobic surfaces. Biomaterials 2006, 27, 4325-4332.

[15] Ruggeri, Z. M.; Mendolicchio, G. L. Adhesion Mechanisms in Platelet Function. Circulation Research 2007, 100, 1673-1685.

[16] Kuharsky, A. L.; Fogelson, A. L. Surface-mediated control of blood coagulation: the role of binding site densities and platelet deposition. Biophysical Journal 2001, 80, 1050-1074.

[17] Beumer, S.; Heijnen, H. F.; Ijsseldijk, M. J.; Orlando, E.; de Groot, P. G.; Sixma, J. J. Platelet adhesion to fibronectin in flow: the importance of von Willebrand factor and glycoprotein Ib. Blood 1995, 86, 3452-3460.

[18] Hindriks, G.; Ijsseldijk, M. J.; Sonnenberg, A.; Sixma, J. J.; de Groot, P. G. Platelet adhesion to laminin: role of Ca2+ and Mg2+ ions, shear rate, and platelet membrane glycoproteins. Blood 1992, 79, 928-935.

[19] Godyna, S.; Diaz-Ricart, M.; Argraves, W. S. Fibulin-1 mediates platelet adhesion via a bridge of fibrinogen. Blood 1996, 88, 2569-2577.

[20] Jurk, K.; Clemetson, K. J.; de Groot, P. G.; Brodde, M. F.; Steiner, M.; Savion, N.; Varon, D.; Sixma, J. J.; Van Aken, H.; Kehrel, B. E. Thrombospondin-1 mediates platelet adhesion at high shear via glycoprotein Ib (GPIb): an alternative/backup mechanism to von Willebrand factor. The FASEB Journal 2003.

[21] Hakim, R. M. Clinical implications of hemodialysis membrane biocompatibility. Kidney Int 1993, 44, 484-494.

[22] Bouré, T.; Vanholder, R. Which dialyser membrane to choose? Nephrology Dialysis Transplantation 2004, 19, 293-296.

[23] Hinrichs, W. L. J.; ten Hoopen, H. W. M.; Engbers, G. H. M.; Feijen, J. In vitro evaluation of heparinized Cuprophan hemodialysis membranes. Journal of Biomedical Materials Research 1997, 35, 443-450.

[24] Cheung, A. K. Biocompatibility of hemodialysis membranes. Journal of the American Society of Nephrology 1990, 1, 150-161.

[25] Cheung, A. K.; Parker, C. J.; Wilcox, L.; Janatova, J. Activation of the alternative pathway of complement by cellulosic hemodialysis membranes. Kidney Int 1989, 36, 257-265.

[26] Hoenich, N. A.; Woffindin, C.; Matthews, J. N. S.; Goldfinch, M. E.; Turnbull, J. Clinical comparison of high-flux cellulose acetate and synthetic membranes. Nephrology Dialysis Transplantation 1994, 9, 60-66.

[27] Clark, W. R.; Gao, D. Properties of Membranes Used for Hemodialysis Therapy. Seminars in Dialysis 2002, 15, 191-195.

[28] Gautham, A.; Muhammed, J. M.; Murugan, M.; Manssor, A. N. Hemodialysis Membranes: Past, Present and Future Trends. Interantional Research Journal of Pharmacy 2013, 4, 16-19.

[29] Bowry, S. K.; Rintelen, T. H. Synthetically Modified Cellulose (SMC): A Cellulosic Hemodialysis Membrane With Minimized Complement Activation. ASAIO Journal 1998, 44.

[30] Daugirdas, J. T.; Bernardo, A. A. Hemodialysis effect on platelet count and function and hemodialysis-associated thrombocytopenia. Kidney Int 2012, 82, 147-157.

[31] Hoenich, N. A.; Woffindin, C.; Stamp, S.; Roberts, S. J.; Turnbull, J. Synthetically modified cellulose: an alternative to synthetic membranes for use in haemodialysis? Biomaterials 1997, 18, 1299-1303.

[32] Falkenhagen, D.; Bosch, T.; Brown, G. S.; Schmidt, B.; Holtz, M.; Baurmeister, U.; Gurland, H.; Klinkmann, H. A Clinical Study on Different Cellulosic Dialysis Membranes. Nephrology Dialysis Transplantation 1987, 2, 537-545.

[33] Hakim, R. M.; Schafer, A. I. Hemodialysis-associated platelet activation and thrombocytopenia. The American Journal of Medicine 1985, 78, 575-580.

[34] Amato, M.; Salvadori, M.; Bergesio, F.; Messeri, A.; Filimberti, E.; Morfini, M. Aspects of biocompatibility of two different dialysis membranes: cuprophane and polysulfone. Int J Artif Organs 1988, 11, 175-80.

[35] Kuwahara, T.; Markert, M.; Wauters, J. P. Biocompatibility aspects of dialyzer reprocessing: a comparison of 3 re-use methods and 3 membranes. Clin Nephrol 1989, 32, 139-43.

[36] Cases, A.; Reverter, J. C.; Escolar, G.; Sanz, C.; Lopez-Pedret, J.; Revert, L.; Ordinas, A. Platelet activation on hemodialysis: influence of dialysis membranes. Kidney Int Suppl 1993, 41, S217-20.

[37] Lehninger, A. L.; Nelson, D. L.; Cox, M. M. Lehninger principles of biochemistry. W.H. Freeman: New York, 2005.

[38] Lesk, A. M. Introduction to protein science : architecture, function, and genomics. Oxford University Press: Oxford; New York, 2004.

[39] Devlin, T. M. Textbook of biochemistry : with clinical correlations. John Wiley & Sons: Hoboken, NJ, 2011.

[40] Lehninger, A. L. Principles of biochemistry. Worth Publishers: 1982.

[41] All about proteins. http://doubledecker27.blogspot.com/2014/10/all-about-protein.html

[42] Hlady, V.; Buijs, J. Protein adsorption on solid surfaces. Current Opinion in Biotechnology 1996, 7, 72-77.

[43] Haynes, C. A.; Norde, W. Globular proteins at solid/liquid interfaces. Colloids and Surfaces B: Biointerfaces 1994, 2, 517-566.

[44] Andrade, J. D. Surface and interfacial aspects of biomedical polymers. Plenum Press: New York, 1985.

[45] Horbett, T. A. Chapter 13 Principles underlying the role of adsorbed plasma proteins in blood interactions with foreign materials. Cardiovascular Pathology 1993, 2, 137-148.

[46] Vroman, L.; Adams, A. L. Findings with the recording ellipsometer suggesting rapid exchange of specific plasma proteins at liquid/solid interfaces. Surface Science 1969, 16, 438-446.

[47] Vroman, L.; Adams, A. L. Identification of rapid changes at plasma–solid interfaces. Journal of Biomedical Materials Research 1969, 3, 43-67.

[48] Vroman, L.; Adams, A. L.; Fischer, G. C.; Munoz, P. C. Interaction of high molecular weight kininogen, factor XII, and fibrinogen in plasma at interfaces. Blood 1980, 55, 156-9.

[49] Zucker, M. B.; Vroman, L. Platelet adhesion induced by fibrinogen adsorbed onto glass. Proc Soc Exp Biol Med 1969, 131, 318-20.

[50] Hirsh, S. L.; McKenzie, D. R.; Nosworthy, N. J.; Denman, J. A.; Sezerman, O. U.; Bilek, M. M. M. The Vroman effect: Competitive protein exchange with dynamic multilayer protein aggregates. Colloids and Surfaces B: Biointerfaces 2013, 103, 395-404.

[51] Keogh, J. R.; Eaton, J. W. Albumin binding surfaces for biomaterials. J Lab Clin Med 1994, 124, 537-45.

[52] Schaller, J. Human blood plasma proteins : structure and function. John Wiley & Sons: Chichester, West Sussex, England; Hoboken, NJ, 2008.

[53] Shang, L.; Wang, Y.; Jiang, J.; Dong, S. pH-Dependent Protein Conformational Changes in Albumin:Gold Nanoparticle Bioconjugates: A Spectroscopic Study. Langmuir 2007, 23, 2714-2721.

[54] Sethuraman, A.; Belfort, G. Protein Structural Perturbation and Aggregation on Homogeneous Surfaces. Biophysical Journal 2005, 88, 1322-1333.

[55] Kim, D. T.; Blanch, H. W.; Radke, C. J. Direct Imaging of Lysozyme Adsorption onto Mica by Atomic Force Microscopy. Langmuir 2002, 18, 5841-5850.

[56] Mrksich, M.; Sigal, G. B.; Whitesides, G. M. Surface Plasmon Resonance Permits in Situ Measurement of Protein Adsorption on Self-Assembled Monolayers of Alkanethiolates on Gold. Langmuir 1995, 11, 4383-4385.

[57] Malmsten, M.; Muller, D.; Lassen, B. Sequential Adsorption of Human Serum Albumin (HSA), Immunoglobulin G (IgG), and Fibrinogen (Fgn) at HMDSO Plasma Polymer Surfaces. J Colloid Interface Sci 1997, 193, 88-95.

[58] Rechendorff, K.; Hovgaard, M. B.; Foss, M.; Zhdanov, V. P.; Besenbacher, F. Enhancement of Protein Adsorption Induced by Surface Roughness. Langmuir 2006, 22, 10885-10888.

[59] Hylton, D. M.; Shalaby, S. W.; Latour, R. A., Jr. Direct correlation between adsorption-induced changes in protein structure and platelet adhesion. J Biomed Mater Res A 2005, 73, 349-58.

[60] Sivaraman, B.; Latour, R. A. The relationship between platelet adhesion on surfaces and the structure versus the amount of adsorbed fibrinogen. Biomaterials 2010, 31, 832-839.

[61] Sivaraman, B.; Latour, R. A. Time-dependent conformational changes in adsorbed albumin and its effect on platelet adhesion. Langmuir 2012, 28, 2745-52.

[62] Sivaraman, B.; Latour, R. A. The adherence of platelets to adsorbed albumin by receptor-mediated recognition of binding sites exposed by adsorption-induced unfolding. Biomaterials 2010, 31, 1036-44.

Chapter 3 Effects of functional groups on the adsorption of blood proteins onto cellulosic surfaces

3.1 Abstract

Polysaccharide-based materials have been widely used in many biomedical applications that involve contact with blood. Protein adsorption occurs early during blood–material contact and affects subsequent interactions. Thus, understanding blood protein adsorption onto polysaccharide surfaces is of great fundamental importance and is critical for the design of novel polysaccharide biomaterials. Interactions between proteins and materials greatly depend on the surface properties of the material, such as hydrophobicity/hydrophilicity and functional groups. In this work, the adsorption behavior of two blood proteins, human serum albumin (HSA) and human serum fibrinogen (HSF), on two polysaccharide materials commonly used for hemodialysis membranes, regenerated cellulose (RC) and cellulose acetate (CA), were investigated by quartz crystal microbalance with dissipation monitoring (QCM-D) and surface plasmon resonance (SPR). Results showed that more HSA adsorbed onto CA than RC surfaces and indicated differences in protein conformation. HSF adsorbed in equal amounts onto the two surfaces. However, a higher water content of the adsorbed HSF layer on the CA surface suggested differences in protein orientation on these two surfaces.

3.2 Introduction

Regenerated cellulose (RC) and cellulose acetate (CA) (Figure 3.1) are two common polysaccharide materials used for hemodialysis membranes. The RC membrane has been used since the time of the first hemodialysis treatment. However, it causes both complement activation and platelet activation, and therefore is not hemocompatible [1]. Complement activation by cellulose surfaces is attributed to the surface hydroxyl groups, which can covalently bind to the complement activation product C3b [2, 3]. Modified cellulosic membranes, CA membranes for example, were designed to reduce complement activation by substituting the hydroxyl groups and suppress covalent binding of complement activation product C3b. CA used for hemodialysis membranes has a degree of substitution (DS) of 2.5 (cellulose diacetate, *e.g.* Diaphan®) or 2.85, cellulose triacetate, *i.e.* on average five or more hydroxyl groups of the cellobiose repeat unit shown in Figure 3.1 are acetylated [4].

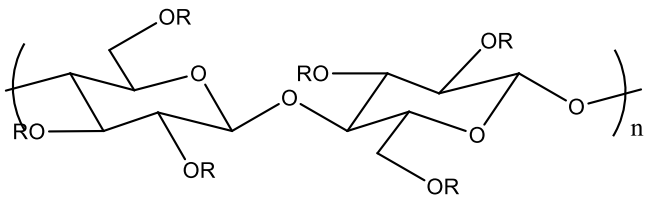

Cellulose: R = H Cellulose Acetate: R = H or $-C(=O)-CH_3$

Figure 3.1 Chemical structure comparisons of cellulose and cellulose acetate

Platelet adhesion is an important consideration when evaluating the blood compatibility of hemodialysis membranes. A decrease in platelet count and platelet aggregation have been observed during hemodialysis treatment, which may cause mild thrombocytopenia problems in some patient cases [5]. Some studies of platelet surface

activation markers have shown that the Cuprophan (RC) membrane causes more platelet activation and aggregation than the CA membrane [5]. The exact mechanism is still unknown.

Protein adsorption is the initial event that occurs when blood contacts the materials. It has been found that platelet adhesion has a specific relationship with albumin and fibrinogen adsorbed onto the surface of a material. While adsorbed fibrinogen is detrimental to the blood compatibility of a material due to the interactions between its specific amino acid sequences with platelet receptors; adsorbed albumin is generally beneficial because it lacks the sequences for platelet binding [6]. Albumin and fibrinogen are the two most abundant proteins in blood. Albumin, with very high concentrations (35–50 g/L), plays important roles in regulating the osmotic pressure and has transporting functions [7]. Fibrinogen (1.5–4.0g/L) is also involved in the blood coagulation process, in which it is converted into fibrin by thrombin [7]. Fundamental studies of the adsorption of both blood proteins on material surfaces are meaningful for exploring the mechanism of platelet adhesion and providing insight for the design of novel biocompatible materials.

The important aspects of protein adsorption that are of interest to study include adsorbed amount, kinetics, and the structure of adsorbed proteins. Many techniques can be used to study protein adsorption, such as surface plasmon resonance (SPR) [8], quartz crystal microbalance with dissipation monitoring (QCM-D)[9], atomic force microscopy (AFM)[10], ellipsometry [11], and circular dichroism (CD)[12]. Among these techniques, SPR and QCM-D are very sensitive for monitoring the adsorbed amount in real time and determining adsorption kinetics.

This study aims to compare differences in adsorption between human serum albumin (HSA) and human serum fibrinogen (HSF) on two cellulose derivatives, RC and CA, by SPR and QCM-D at conditions that imitate the hemodialysis process, i.e. normal blood level concentrations for each protein in phosphate buffered saline (pH = 7.4) and a temperature of 37°C. This study is expected to provide insights that will aid in the design of novel cellulose derivatives for hemodialysis membrane applications.

3.3 Experimental section

3.3.1 Materials

Deionized (DI) water with a resistivity of 18.2 MΩ·cm was obtained from a Millipore Direct-Q 5 Ultrapure water systems. Trimethylsilyl cellulose (DS = 2.71) was prepared by methods described in the literature [13]. CA (CA-398-30, nominal acetyl and hydroxyl contents of 39.8 and 3.5 wt %, respectively) was provided by the Eastman Chemical Company. The measured DS (from the ^{1}H NMR spectrum, Appendix A) was 2.6, which was slightly higher than the DS calculated from the nominal acetyl and hydroxyl contents of 2.45. (It should be pointed out that the CA used in this study likely contained trace amounts of lignin and hemicellulose because it was presumably derived from wood pulp, whereas CA used for commercial hemodialysis membranes is derived from cotton to avoid such contamination [14].) 1,4-Dioxane (99+%, stabilized) was purchased from Acros Organics. Phosphate buffered saline (1X, pH = 7.4), aqueous ammonia (28.9% w/w), hydrogen peroxide (34-37% w/w), and hydrochloric acid (37.4%, w/w) were purchased from Fisher Scientific. Human serum albumin (96+%) and human serum fibrinogen (90+%, clottable) were purchased from Sigma-Aldrich.

3.3.2 Surface preparation

QCMD sensors with a fundamental resonant frequency of 5 MHz, bought from Q-sense AB, and SPR sensors, bought from Reichert, were used as the substrates for thin films. Both sensors have gold-coated surfaces, which were cleaned by exposure to UV/ozone for 20 min, followed by immersion in a boiling solution of 1:1:5 (v/v/v) NH_4OH: H_2O_2: DI water at 80°C for 1h. Finally, the gold surfaces of the sensors were rinsed with large amounts of DI water and dried with nitrogen gas.

RC surfaces were prepared by first spincoating a 10 g/L trimethylsilyl cellulose (TMSC) solution in toluene on the cleaned gold surfaces with at a spinning speed of 2500 rpm for 1 min (WS-400A-6NPP-Lite, Laurell Technologies). Then, the TMSC films were exposed to the vapor of aqueous 10% w/w hydrochloric acid for 2 min to obtain RC films [15]. RC surfaces were heated in a vacuum oven at 65 °C for 2h.

CA was dissolved in 1,4-dioxane to form a 0.5% w/v solution. The solution was filtered through a 0.45 μm syringe filter (Whatman, Ltd) and sonicated prior to use. The CA solution was spincoated onto cleaned gold surfaces with a spinning speed of 2500 rpm for 1 min (WS-400A-6NPP-Lite, Laurell Technologies). CA surfaces were heated in a vacuum oven at 65 °C for 2h.

3.3.3 Surface characterization by AFM

All surfaces were characterized by AFM imaging with an Asylum Research MFP-3D-BIO atomic force microscope. Samples were scanned in air under ambient conditions in tapping mode with OMCL-AC160TS standard silicon probes (Olympus Corp.) Height images are reported without any image processing. Root mean square (RMS) roughnesses of the surfaces were obtained from 5 μm × 5 μm area in triplicate.

3.3.4 Surface plasmon resonance (SPR) measurements

The adsorption behavior of the blood proteins on the surfaces was studied by SPR (SR7000, Reichert Inc.). Gold-coated SPR sensors with RC or CA thin films were placed into the flow cell. A laser diode with an emission wavelength of 780 nm was used as the light source. Degassed protein or buffer solutions were pumped into the flow cell via Teflon tubing at a rate of 0.2 mL/min and a temperature of 37°C by a cartridge pump (Masterflex). The adsorption experiments were performed at least three times.

In SPR measurements, changes in resonant angle ($\Delta\theta_{sp}$) due to protein adsorption and desorption are directly detected by the SPR sensor. The surface concentration (Γ_{SPR}) can be calculated from $\Delta\theta_{sp}$ with the equation of de Feijter *et al.* [16]:

$$\Gamma_{SPR} = \Delta\theta_a \left(\frac{1}{d\theta/dL}\right)\left(\frac{n_s - n_b}{dn/dc}\right)$$

$$\Delta\theta_a = \Delta\theta_{sp} - c\left(\frac{d\theta_{sp}}{dc}\right) = \Delta\theta_{sp} - c\left(\frac{d\theta_{sp}}{dn}\frac{dn}{dc}\right)$$

where $\Delta\theta_a$ is the corrected resonant angle change obtained by subtracting the contribution of bulk refractive index changes in the dielectric medium from the observed $\Delta\theta_{sp}$. c is the bulk concentration of protein solution (40 mg/mL for HSA and 3 mg/mL for HSF). $d\theta_{sp}/dn$ is an instrument specific constant obtained via the calibration of the instrument with ethylene glycol standards (61.5 deg). dn/dc is the refractive index increment of the protein (0.188 mL/g for both HSA and HSF)[17]. $d\theta/dL$ is the change in resonant angle with respect to the unit change in adsorbed layer thickness modeled by the Fresnel equations (0.042 deg/nm) [18]. n_s is the refractive index of the substrate (1.45 for RC and 1.49 for CA) [19, 20]. n_b is the refractive index of the buffer solution (1.345 for PBS).

3.3.5 Quartz crystal microbalance with dissipation (QCM-D) monitoring

The adsorption of the proteins on the surfaces was also studied by QCM-D (Q-Sense E4). The gold-coated QCM-D sensor crystals with RC or CA thin films were placed in QCM-D flow modules. Protein and buffer solutions were pumped into the flow modules by a cartridge pump (ISMATEC-ISM935) at a rate of 0.2 mL/min and a temperature of 37°C. The changes of both quartz crystal oscillation frequency (Δf) and dissipation factor (ΔD) at 5 overtones (n = 3, 5, 7, 9, 11) were monitored simultaneously. The adsorption experiments were performed at least three times.

The QCM-D is very sensitive to the change of surface mass (Δm), which is related to the frequency shift (Δf). For rigid and homogeneous films, there is a linear relationship between the surface concentration Γ_{QCM} and (Δf/n) according to the Sauerbrey equation for a given overtone (n):

$$\Gamma_{QCM} = -C\left(\frac{\Delta f}{n}\right)$$

where C is the mass sensitivity constant (17.7ng·cm^{-2}·Hz^{-1}) for the crystals with a resonant frequency of 5 MHz. The linear relationship does not hold for flexible or soft films. The criterion for rigidity of the adsorbed layer used in this study is that ΔD/(Δf/n) is less than 1×10^{-7}.

Since the Δf represents the total surface mass change, including the mass of adsorbed proteins and the surrounding coupled water, the water content of the adsorbed layer can be calculated by combining the information of Γ_{SPR} and Γ_{QCM}:

$$Water\ content = \left(\frac{\Gamma_{QCM} - \Gamma_{SPR}}{\Gamma_{QCM}}\right)\times 100\%$$

It should be noted that the calculated water content above is not a simple measure of the entrapped water in the adsorbed protein. The water-related mass change measured by QCM includes the mass increase due to the water molecules that are coupled with the adsorbed protein ($\Delta m_{coupled}$) and the mass decrease due to the exclusion of water at the protein–surface interface ($\Delta m_{p\text{-}s}$) as well as the interface between adjacent protein molecules ($\Delta m_{p\text{-}p}$). Thus, the total water-related mass change can be expressed as

$$\Delta m_{total} = \Delta m_{coupled} - \Delta m_{p\text{-}s} - \Delta m_{p\text{-}p}$$

$\Delta m_{coupled}$ may depend on the conformation of the adsorbed protein. $\Delta m_{p\text{-}s}$ depends on the area occupied by the adsorbed protein and the thickness of the water layer on the surface. While the former is related to the conformation and orientation of the adsorbed protein (*e.g.* end on *versus* side on); the latter depends on the hydrophobicity of the surface. A hydrophobic surface has a thinner water layer than a hydrophilic one, resulting in a smaller mass decrease per unit area due to water displacement. Finally, $\Delta m_{p\text{-}p}$ depends on the proximity and packing of the protein molecules on the surface.

3.4 Results and discussion

3.4.1 AFM characterization of CA and RC surfaces

Preparation of homogenous surfaces is critical to adsorption experiments. The morphologies of both CA and RC films spincoated onto gold surface were investigated by AFM. Representative height images of the films are shown in Figure 3.2. Both films are homogenous. The RMS surface roughnesses calculated from 5 μm × 5 μm areas were 1.8 ± 0.4 and 1.2 ± 0.2 nm for CA and RC, respectively.

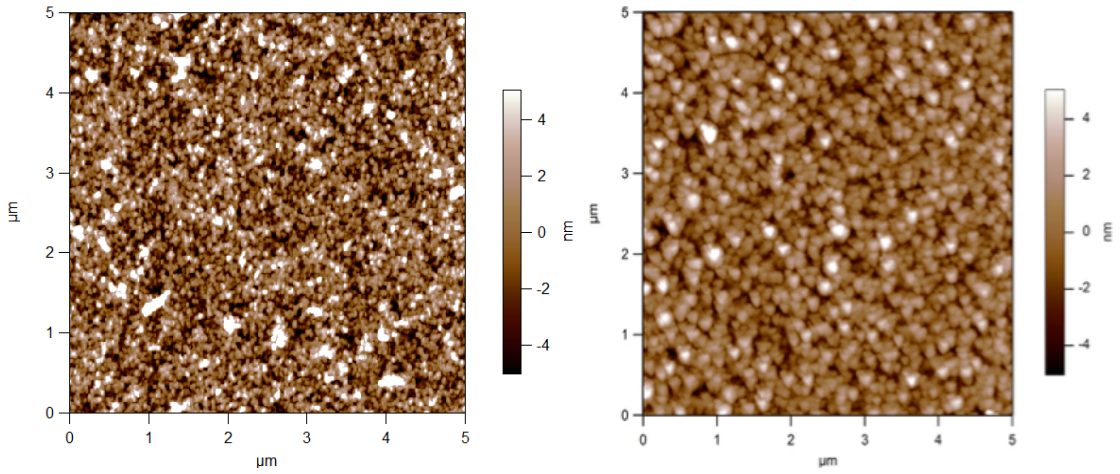

Figure 3.2 Representative AFM height images of CA (left) and RC (right) surfaces

3.4.2 Adsorption of HSA onto CA and RC surfaces

Figure 3.3 shows representative $\Delta\theta_{sp}$ curves for HSA adsorption onto CA and RC surfaces. The surfaces were equilibrated in PBS to obtain a baseline. After 5 min, HSA in PBS at a concentration of 40 mg/mL, mimicking a normal HSA blood concentration, was injected into the chamber, resulting in immediate protein adsorption. After a flow of HSA solution for around 20 min, a plateau was observed, indicating an equilibrium between adsorption and desorption processes. At t = 25 min, PBS was injected again to wash reversibly adsorbed HSA from the surfaces, leaving only irreversibly adsorbed proteins. The two $\Delta\theta_{sp}$ *versus* time curves for HSA adsorption onto RC and CA showed no significant differences.

A comparison of representative $(\Delta f/n)$ curves for CA and RC is presented in Figure 3.4A. The experimental process is the same as described above; however, the adsorption curves obtained by QCM-D for the two cellulosic surfaces are obviously different. The greater decrease in $(\Delta f/n)$ upon protein adsorption onto CA (Figure 3.4A) signifies that the increase of surface mass on CA is much larger than that on RC.

Contrary to the $\Delta\theta_{sp}$ change measured by SPR, which reflect only the mass of the adsorbed protein, the surface mass change measured by QCM-D involves both the adsorbed protein and the water associated with the adsorbed layer. The larger dissipation factor change for adsorption onto CA (Figure 3.4B) indicated that the adsorbed HSA layer on CA was more flexible than that on RC. Seeing that $-\Delta D/(\Delta f/n)$ for the irreversibly adsorbed layer was on the order of 10^{-7}, the Sauerbrey equation was used to estimate the surface mass of the irreversibly adsorbed HSA layer with the associated water. The surface concentrations of HSA calculated from both SPR (Γ_{SPR}) and QCM (Γ_{QCM}), a measure of rigidity ($-\Delta D/(\Delta f/n)$, and estimated water contents for both CA and RC in Table 3.1.

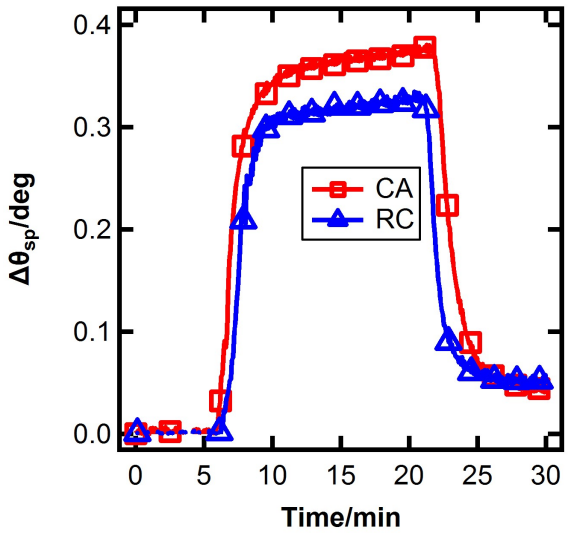

Figure 3.3 Representative SPR curves for HSA adsorption onto CA (□) and RC (△)

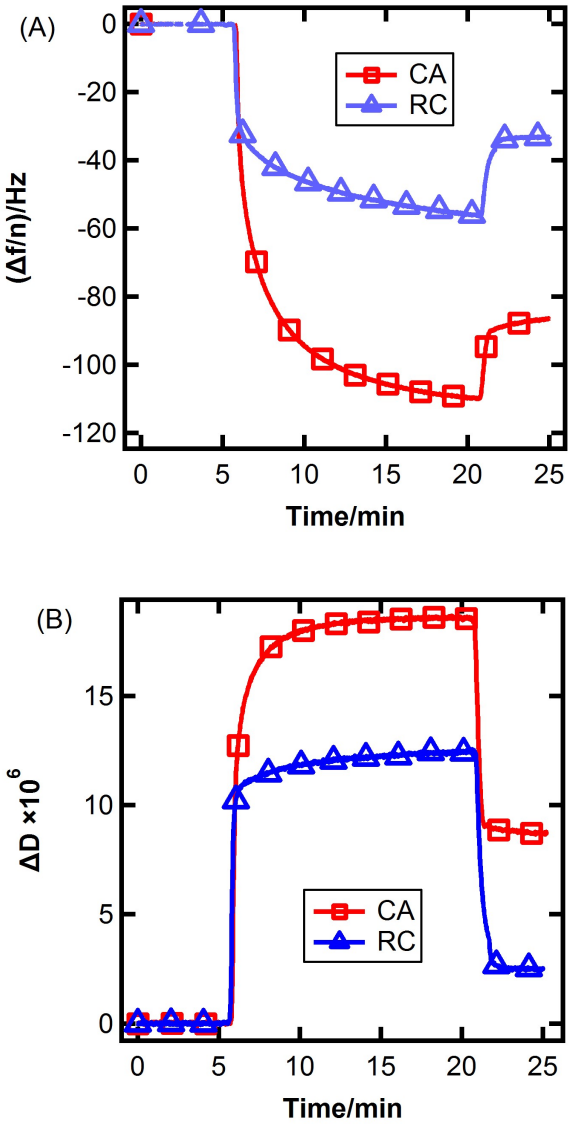

Figure 3.4 Representative QCM-D (A) frequency change and (B) dissipation change curves for HSA adsorption onto CA (□) and RC (△) (5th overtone)

Table 3.1 Surface concentration and water content of adsorbed HSA layers

	CA	RC
$\boldsymbol{\Gamma_{SPR}}$(mg /m^2)	0.83 ± 0.04	0.69 ± 0.05
–ΔD/(Δf/n)($\times 10^{-7}$)	1.00 ± 0.06	0.77 ± 0.02
$\boldsymbol{\Gamma_{QCM}}$(mg /m^2)	14.20 ± 1.87	1.27 ± 0.13
Water Content (%)	94.1 ± 0.9	89.2 ± 1.3

HSA is an asymmetric protein with heart-shaped structure. Many studies have reported different sizes for HSA in solution. Here, a globular shape with a diameter of 7 nm was assumed for estimation of the surface concentration at full surface coverage [21, 22]. The unit surface contact area for an adsorbed HSA molecule is approximately 49 nm^2, assuming that no conformational change happens upon adsorption; thus, the full coverage surface concentration is approximately 2.3 mg/m^2. The surface concentrations of adsorbed HSA on CA and RC from SPR data were 0.83 ± 0.04 mg/m^2 and 0.69 ± 0.05 mg/m^2, respectively. Both concentrations are of the same order of magnitude, but below full theoretical surface coverage, which suggests HSA forms monolayers on these surfaces.

Both HSA layers contained large amounts of associated water. The HSA layer on the more hydrophobic CA surface had a higher water content (~ 94%) than that on the more hydrophilic RC surface (~ 89%). As discussed in Section 3.3.5, a larger Δm_{total} could be due to a larger $\Delta m_{\text{coupled}}$ (related to the protein conformation), a smaller $\Delta m_{\text{p-s}}$ (smaller binding area or higher surface hydrophobicity), and a smaller $\Delta m_{\text{p-p}}$ (low packing density). The larger water content of the adsorbed HSA layer on the CA surface

is consistent with a higher surface hydrophobicity of CA because it signifies a small $\Delta m_{p\text{-}s}$. The low measured surface concentration relative to the theoretical saturation surface concentration might indicate that the protein molecules are not tightly packed and the contribution of $\Delta m_{p\text{-}p}$ to Δm_{total} is small.

Being a measure of rigidity, the higher $-\Delta D/(\Delta f/n)$ value for CA shows that the HSA layer on CA is more flexible ($\sim 1\times10^{-7}$) than that on RC ($\sim 0.77\times10^{-7}$). Thus, the difference in water content may also be due to different HSA conformations or orientations ($\Delta m_{coupled}$). The study by Roach *et al.* has shown that bovine serum albumin loses some of its α-helical character and experiences an increase in its random coil structure component on a hydrophobic surface [9]. The unfolding process caused by the hydrophobic surface could result in different HSA conformations with different water contents on the two surfaces.

3.4.3 Adsorption of HSF onto CA and RC surfaces

For HSF adsorption experiments, an HSF concentration in PBS of 3 mg/mL was used, mimicking a normal HSF blood concentration. Representative SPR and QCM-D data for HSF adsorption onto CA and RC surfaces are shown in Figure 3.5 and Figure 3.6.

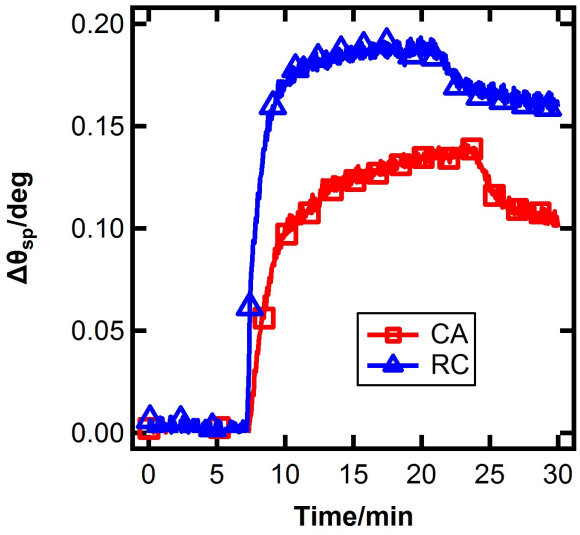

Figure 3.5 Representative SPR curves for HSF adsorption onto CA (□) and RC (△)

A

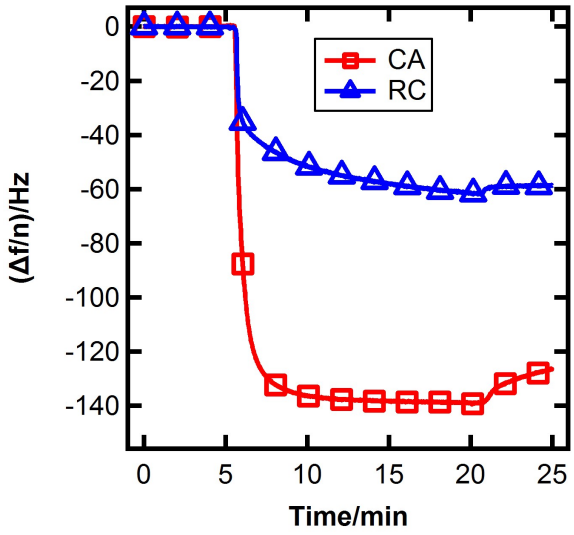

B

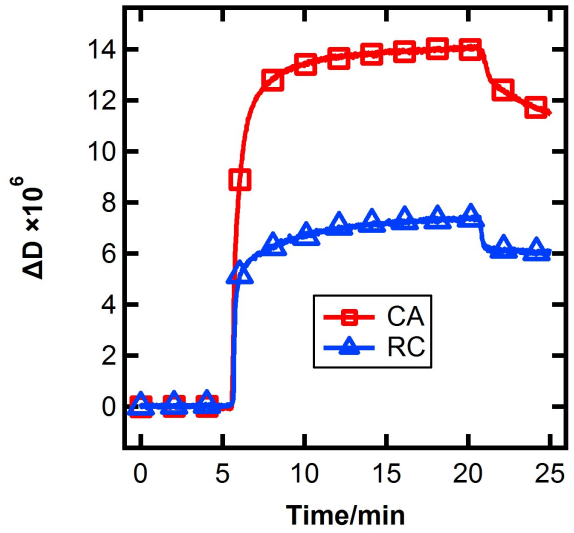

Figure 3.6 Representative QCM-D (A) frequency change and (B) dissipation change curves for HSF adsorption onto CA (□) and RC (△) (5th overtone)

Table 3.2 Surface concentration and water content of adsorbed HSF layers

	CA	RC
$\boldsymbol{\Gamma_{SPR}}$(mg/m^2)	1.98 ± 0.07	2.08 ± 0.12
–ΔD/(Δf /n)(×10 $^{-7}$)	0.91 ± 0.01	0.92 ± 0.10
$\boldsymbol{\Gamma_{QCM}}$(mg/m^2)	4.50 ± 0.18	2.13 ± 0.11
Water Content (%)	91.3 ± 0.4	76.4 ± 4.4

The surface concentrations of HSF molecules from SPR data, the surface masses of the aqueous HSF layers from QCM-D data, and the calculated water contents for both CA and RC are summarized in Table 3.2. HSF is a rod-shaped protein with dimensions of 47.5 × 9 × 6 nm [23]. There are two possible orientations for adsorbed HSF molecules: side-on (with the long axis parallel to the surface) with contact areas of 427.5 and 285 nm^2 for the wider and narrower side, respectively, or end-on (with the long axis perpendicular to the surface) with a contact area of 54 nm^2. Thus, the saturation concentration for pure side-on adsorption ranges from 1.32 (all wide-side-on) to 1.98 mg/m^2 (all narrow-side-on) and that for pure end-on adsorption is 10.46 mg/m^2.

The surface concentrations of HSF adsorbed onto CA and RC from SPR data were 1.98 ± 0.07 mg/m^2 and 2.08 ± 0.12 mg/m^2, respectively (Table 3.2). The difference was not statistically significant. It can therefore be concluded that HSF adsorbs in equal amounts onto CA and RC surfaces. The surface concentration of adsorbed HSF molecules was close to the saturation concentration for pure side-on adsorption. While this result would be in agreement with a closely packed side-on monolayer, the high degree of order (perfect alignment of the rod-shaped molecules and end-to-end contact of

collinear neighbors) required to reach the saturation concentration for pure side-on adsorption is unlikely to be achieved under the conditions of these adsorption experiments. Thus, the HSF surface concentrations measured by SPR more likely suggest at least some degree of multilayer formation or end-on adsorption.

According to the study by Roach *et al.* [9], bovine serum fibrinogen undergoes less extensive conformational changes upon surface adsorption than bovine serum albumin. Nevertheless, the adsorption behavior of bovine serum fibrinogen was found to be more complex. The authors proposed a stepwise adsorption process with initial side-on adsorption followed by reorientation of the protein molecules to an end-on orientation, enabling additional protein adsorption. The driving force for the reorientation was thought to be stronger hydrophobic interactions between adjacent end-on fibrinogen molecules than between fibrinogen molecules and the surface. Hydrophobic protein–surface interactions are smaller on hydrophilic surfaces than hydrophobic surfaces. Therefore, the driving force for HSF reorientation would be greater on the hydrophilic RC surface relative to the hydrophobic CA surface.

Although the observed adsorbed amount and flexibility of the protein layers are almost the same for the two surfaces, the adsorbed HSF layer on the CA surface contained significantly more water (~91%) than the layer on the RC surface (~76%). As discussed in Section 3.3.5, a larger Δm_{total} could be due to a larger $\Delta m_{coupled}$ (related to the protein conformation), a smaller $\Delta m_{p\text{-}s}$ (smaller binding area or higher surface hydrophobicity), and a smaller $\Delta m_{p\text{-}p}$ (low packing density). Under the assumption that HSF is rigid and undergoes no significant conformational change upon adsorption, the influence of $\Delta m_{coupled}$ on Δm_{total} would be negligible. The influence of $\Delta m_{p\text{-}s}$, however, is

complex. While on the more hydrophobic CA surface the larger binding area of the preferred side-on orientation would result in a greater $\Delta m_{p\text{-}s}$, the smaller thickness of the excluded water layer would cause a smaller $\Delta m_{p\text{-}s}$ than on the more hydrophilic RC surface. One possible explanation for the dramatic difference in water contents could be different HSF orientations. Considering that a saturated side-on monolayer on the two surfaces is unlikely, HSF molecules may form side-on multilayers on the more hydrophobic CA surface, trapping a large amount of water, whereas they may form clusters of end-on adsorbed HSF molecules on the more hydrophilic RC surface, causing a greater $\Delta m_{p\text{-}p}$. than on the CA surface.

Interestingly, on the CA surface, HSF adsorption was found to be slowly reversible. Upon washing with PBS, after an initial rapid desorption process, a continuous gradual mass loss was observed for HSF on CA (Figure 3.7). This behavior was different from that observed for HSA and could be due to slow desorption of weakly bound molecules. The fact that this behavior was not observed on the RC surface suggested that some HSF molecules bound more strongly to RC surface than the CA surface. The observed desorption could be an indication of loosely bound HSF, possibly with end-on orientation or stacked in a higher order adsorption layer, on CA.

A

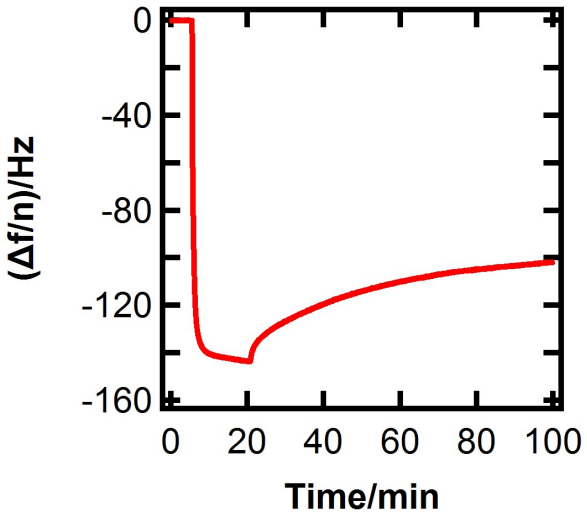

B

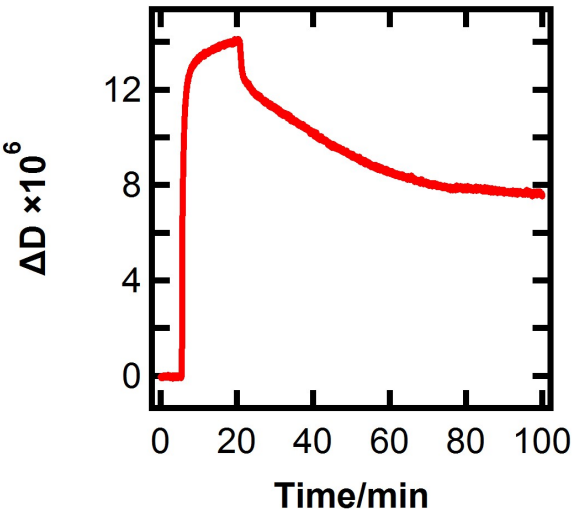

Figure 3.7 Representative QCM-D (A) frequency change and (B) dissipation change curves for HSA adsorption onto CA (5th overtone)

3.5 Conclusions

Given the facts that blood protein adsorption plays a critical role in the hemocompatibility of materials and CA hemodialysis membranes cause less platelet adhesion and activation than RC hemodialysis membranes, the adsorption behavior of two blood proteins, HSA and HSF, on CA and RC surfaces was studied to explore the effect of acetyl substitution on protein adsorption. It was found that HSA adsorption, commonly regarded as beneficial for hemocompatibility, was greater on the hydrophobic CA surface than the hydrophilic RC surface. The HSA layer on the CA surface was more flexible and contained more water than the HSA layer on the RC surface possibly because of different HSA conformations on the two surfaces. HSF adsorbed in equal amounts onto the hydrophobic CA and hydrophilic RC surface. HSF adsorption onto CA surfaces was accompanied by a larger change in coupled water than HSF adsorption onto RC surfaces, possibly because of different HSF orientations on the two surfaces. Gradual HSF desorption was observed on the CA but not the RC surface, suggesting a higher affinity of HSF for the RC surface.

3.6 Acknowledgements

This material is based upon work supported in part by the National Science Foundation under grant number DMR-0907567. Moreover, this work was supported in part by the Virginia Agricultural Experiment Station and the USDA National Institute of Food and Agriculture, Hatch/Multi State project 1002269 and grant number 2010-65504-20429. Partial funding from the Macromolecules and Interfaces Institute is also acknowledged.

3.7 References

[1] Hinrichs, W. L. J.; ten Hoopen, H. W. M.; Engbers, G. H. M.; Feijen, J. In vitro evaluation of heparinized Cuprophan hemodialysis membranes. Journal of Biomedical Materials Research 1997, 35, 443-450.

[2] Cheung, A. K. Biocompatibility of hemodialysis membranes. Journal of the American Society of Nephrology 1990, 1, 150-161.

[3] Cheung, A. K.; Parker, C. J.; Wilcox, L.; Janatova, J. Activation of the alternative pathway of complement by cellulosic hemodialysis membranes. Kidney Int 1989, 36, 257-265.

[4] Hoenich, N. A.; Woffindin, C.; Matthews, J. N. S.; Goldfinch, M. E.; Turnbull, J. Clinical comparison of high-flux cellulose acetate and synthetic membranes. Nephrology Dialysis Transplantation 1994, 9, 60-66.

[5] Daugirdas, J. T.; Bernardo, A. A. Hemodialysis effect on platelet count and function and hemodialysis-associated thrombocytopenia. Kidney Int 2012, 82, 147-157.

[6] Liu, X.; Yuan, L.; Li, D.; Tang, Z.; Wang, Y.; Chen, G.; Chen, H.; Brash, J. L. Blood compatible materials: state of the art. Journal of Materials Chemistry B 2014, 2, 5718-5738.

[7] Schaller, J. Human blood plasma proteins : structure and function. John Wiley & Sons: Chichester, West Sussex, England; Hoboken, NJ, 2008.

[8] Mrksich, M.; Sigal, G. B.; Whitesides, G. M. Surface Plasmon Resonance Permits in Situ Measurement of Protein Adsorption on Self-Assembled Monolayers of Alkanethiolates on Gold. Langmuir 1995, 11, 4383-4385.

[9] Roach, P.; Farrar, D.; Perry, C. C. Interpretation of Protein Adsorption: Surface-Induced Conformational Changes. Journal of the American Chemical Society 2005, 127, 8168-8173.

[10] Cacciafesta, P.; Humphris, A. D. L.; Jandt, K. D.; Miles, M. J. Human Plasma Fibrinogen Adsorption on Ultraflat Titanium Oxide Surfaces Studied with Atomic Force Microscopy. Langmuir 2000, 16, 8167-8175.

[11] Malmsten, M.; Muller, D.; Lassen, B. Sequential Adsorption of Human Serum Albumin (HSA), Immunoglobulin G (IgG), and Fibrinogen (Fgn) at HMDSO Plasma Polymer Surfaces. J Colloid Interface Sci 1997, 193, 88-95.

[12] Sivaraman, B.; Fears, K. P.; Latour, R. A. Investigation of the Effects of Surface Chemistry and Solution Concentration on the Conformation of Adsorbed Proteins Using an Improved Circular Dichroism Method. Langmuir 2009, 25, 3050-3056.

[13] Rivera-Armenta, J. L.; Heinze, T.; Mendoza-Martínez, A. M. New polyurethane foams modified with cellulose derivatives. European Polymer Journal 2004, 40, 2803-2812.

[14] Bouré, T.; Vanholder, R. Which dialyser membrane to choose? Nephrology Dialysis Transplantation 2004, 19, 293-296.

[15] Kontturi, E.; Thüne, P. C.; Niemantsverdriet, J. W. Cellulose Model SurfacesSimplified Preparation by Spin Coating and Characterization by X-ray Photoelectron Spectroscopy, Infrared Spectroscopy, and Atomic Force Microscopy. Langmuir 2003, 19, 5735-5741.

[16] De Feijter, J. A.; Benjamins, J.; Veer, F. A. Ellipsometry as a tool to study the adsorption behavior of synthetic and biopolymers at the air–water interface. Biopolymers 1978, 17, 1759-1772.

[17] Malmsten, M. Ellipsometry Studies of Protein Adsorption at Lipid Surfaces. J Colloid Interface Sci 1994, 168, 247-254.

[18] Kittle, J. D.; Du, X.; Jiang, F.; Qian, C.; Heinze, T.; Roman, M.; Esker, A. R. Equilibrium Water Contents of Cellulose Films Determined via Solvent Exchange and Quartz Crystal Microbalance with Dissipation Monitoring. Biomacromolecules 2011, 12, 2881-2887.

[19] Kaya, A.; Du, X.; Liu, Z.; Lu, J. W.; Morris, J. R.; Glasser, W. G.; Heinze, T.; Esker, A. R. Surface Plasmon Resonance Studies of Pullulan and Pullulan Cinnamate Adsorption onto Cellulose. Biomacromolecules 2009, 10, 2451-2459.

[20] http://www.matbase.com/material-categories/natural-and-synthetic-polymers/thermoplastics/engineering-polymers/material-properties-of-synthetic-cellulose-acetate-ca.html - properties

[21] Kiselev, M. A.; Gryzunov Iu, A.; Dobretsov, G. E.; Komarova, M. N. Size of a human serum albumin molecule in solution. Biofizika 2001, 46, 423-7.

[22] Ferrer, M. L.; Duchowicz, R.; Carrasco, B.; de la Torre, J. G.; Acuna, A. U. The conformation of serum albumin in solution: a combined phosphorescence depolarization-hydrodynamic modeling study. Biophys J 2001, 80, 2422-30.

[23] ATR-FTIR measurements of albumin and fibrinogen adsorption: Inert versus calcium phosphate ceramics. Journal of Biomedical Materials Research Part A 2015, n/a.

Chapter 4 Effects of acetyl group content on adsorption of human serum albumin onto cellulose acetate surfaces

4.1 Abstract

It is commonly believed that the presence of albumin layers is beneficial to the hemocompatibility of biomaterials by minimizing platelet adhesion. Previous studies have shown that the modification of cellulose with acetyl groups decreases platelet adhesion. In the design of novel cellulose derivatives, the degree of substitution (DS) with functional groups requires critical consideration. This studies aims to explore the relationship between the DS of cellulose acetate (CA) and the adsorption behavior of HSA to provide insight into the influence of surface functional groups. The results suggest that the DS value of the CA material is not the main factor governing the adsorbed amount of HSA but that it has a strong effect on the water content of the HSA layer, possibly by influencing HSA conformation.

4.2 Introduction

Serum albumin is the most abundant protein in human blood plasma. It is produced in the liver and plays important roles in maintaining the osmotic pressure and transporting molecules with low water solubility, such as hormones, fatty acids, and drugs [1]. Albumin is a single-chain, heart-shaped molecule with a molar mass of around 67 kDa [1]. The normal level of serum albumin in human plasma varies from 35 to 50 g/L [1].

During the contact of blood with a material surface, adsorption of blood proteins onto the surface is the initial event. The phenomenon known as the Vroman effect predicts the sequential adsorption of blood proteins, specifically that proteins with highest mobility arrive at and adsorb onto the surface first and are subsequently replaced by proteins with lower mobility and higher affinity [2]. Typically, proteins with high mobility have a low molecular weight and high concentration in the blood. The sequence of initial adsorption under stagnant conditions is: albumin, globulin, and fibrinogen [2]. Fibrinogen may be displaced by higher molecular weight proteins, such as coagulation factor XII or high-molecular-weight kininogen, which participate in the initiation of platelet adhesion and blood coagulation events [2]. Previous studies have shown that once albumin adsorbs, Vroman displacement of it by other blood proteins is minimal.[3] This phenomenon seems to conflict with in vivo observations, which reflect a more complicated environment in which interactions among blood proteins need to be considered [3].

The adsorption of human serum albumin (HSA), generally believed beneficial, has been found closely related to platelet adhesion. Because HSA does not possess any known amino acid sequences for platelet binding receptors, the HSA layer is thought to block platelet–material interaction [4]. As a result, it is used for coating of some biomaterial surfaces to improve hemocompatibility. However, one recent study has shown that once albumin undergoes a critical degree of unfolding, around 34% loss in α-helical structure, platelet adhesion increases with increasing degree of unfolding, similar to that observed with fibrinogen [3]. The unfolding of albumin only happens with dilute

albumin solution ($c < 10$ mg/mL). Under physiological conditions ($c \approx 40$ mg/mL), adsorption-induced unfolding of albumin has not been observed [3].

Protein adsorption is a complicated process, involving interactions among surfaces, proteins, and the environment. In the design of polysaccharide materials for blood contacting applications, the degree of substitution (DS) with functional groups has a great effect on the surface properties of the polysaccharide materials, such as chemical composition, morphology, surface charge, and hydrophilicity/hydrophobicity. Thus, it may affect the interaction between material surfaces and proteins. Some studies shows that the modification of cellulose with acetyl groups may decrease the platelet adhesion on the surface, thus improve the hemocompatibility [5]. In this study, we are interested in the relationship between the density of acetyl groups on cellulose acetate (CA) and the adsorption behavior of HSA, which can possibly provide valuable insights for the design of hemocompatible biomaterials.

4.3 Experimental section

4.3.1 Materials

Deionized (DI) water with a resistivity of 18.2 MΩ·cm was obtained from a Millipore Direct-Q 5 Ultrapure water systems. CA materials with different DS (CA-320S, CA-398-30, CA436-80s) were provided by the Eastman Chemical Company. 1,4-Dioxane (99+%, stabilized) was purchased from Acros Organics. Phosphate buffered saline (1X, pH=7.4), aqueous ammonia (28.9% w/w), hydrogen peroxide (34-37% w/w), and hydrochloric acid (37.4%, w/w) were purchased from Fisher Scientific. Human serum albumin (96+%) was purchased from Sigma-Aldrich.

4.3.2 Surface preparation

Quartz crystal microbalance with dissipation monitoring (QCM-D) sensors with a fundamental resonant frequency of 5 MHz, bought from Q-sense AB, and surface plasmon resonance (SPR) sensors, bought from Reichert, were used as the substrates for thin film studies. Both sensors have gold-coated surfaces, which were cleaned by exposure to UV/ozone for 20 min, followed by immersion in a boiling solution of 1:1:5 (v/v/v) NH_4OH:H_2O_2:DI water at 80°C for 1 h. Finally, the gold surface of the sensors were rinsed with large amounts of DI water and dried in a nitrogen gas flow.

CA materials with different DS were dissolved in 1,4-dioxane to form 0.5% w/v solutions. The solutions were filtered through 0.45 μm syringe filters (Whatman, Ltd) and sonicated prior to use. The CA solutions were spincoated onto cleaned gold surfaces with a spinning speed of 2500 rpm for 1 min (WS-400A-6NPP-Lite, Laurell Technologies). CA surfaces were heated in a vacuum oven at 65 °C for 2 h.

4.3.3 Surface characterization by AFM

All surfaces were characterized by AFM imaging with an Asylum Research MFP-3D-BIO atomic force microscope. Samples were scanned in air under ambient conditions in tapping mode with OMCL-AC160TS standard silicon probes (Olympus Corp.) Height images are reported without any image processing. Root mean square (RMS) roughnesses of the surfaces were obtained from 2 μm × 2 μm areas in triplicate.

4.3.4 Surface plasmon resonance (SPR) measurements

The adsorption behavior of the blood proteins on the surfaces was studied by SPR (SR7000, Reichert Inc.). Gold-coated SPR sensors with CA thin films were placed into the flow cell. A laser diode with an emission wavelength of 780 nm was used as the light

source. Degassed protein or buffer solutions were pumped into the flow cell via Teflon tubing by a cartridge pump (Masterflex) at a rate of 0.2 mL/min and a temperature of 37°C. The adsorption experiments were performed at least three times.

In SPR measurements, changes in resonant angle ($\Delta\theta_{sp}$) due to protein adsorption and desorption are directly detected by the SPR sensor. The surface concentration (Γ_{SPR}) can be calculated from $\Delta\theta_{sp}$ with the equation of de Feijter *et al.* [6]:

$$\Gamma_{SPR} = \Delta\theta_a \left(\frac{1}{d\theta/dL}\right)\left(\frac{n_s - n_b}{dn/dc}\right)$$

$$\Delta\theta_a = \Delta\theta_{sp} - c\left(\frac{d\theta_{sp}}{dc}\right) = \Delta\theta_{sp} - c\left(\frac{d\theta_{sp}}{dn}\frac{dn}{dc}\right)$$

where $\Delta\theta_a$ is the corrected resonant angle change obtained by subtracting the contribution of bulk refractive index changes in the dielectric medium from the observed $\Delta\theta_{sp}$. c is the bulk concentration of protein solution (40 mg/mL). $d\theta_{sp}/dn$ is an instrument specific constant obtained via the calibration of the instrument with ethylene glycol standards (61.5 deg). dn/dc is the refractive index increment of the protein (0.188 mL/g) [7]. $d\theta/dL$ is the change in resonant angle with respect to the unit change in adsorbed layer thickness modeled by the Fresnel equations (0.042 deg/nm) [8]. n_s is the refractive index of the substrate (1.49 for all three CA surfaces) [9, 10]. n_b is the refractive index of the buffer solution (1.345 for PBS).

4.3.5 Quartz crystal microbalance with dissipation (QCM-D) monitoring

The adsorption of albumin onto the CA surfaces was also studied by QCM-D (Q-Sense E4). The gold-coated QCM-D sensor crystals with CA thin films were placed in QCM-D flow modules. Protein and buffer solutions were pumped into the flow modules by a cartridge pump (ISMATEC-ISM935) at a rate of 0.2 mL/min and a temperature of

37 °C. The changes of both quartz crystal oscillation frequency (Δf) and dissipation factor (ΔD) at 5 overtones (n = 3, 5, 7, 9, 11) were monitored simultaneously. The adsorption experiments were performed at least three times.

The QCM-D is very sensitive to the change of surface mass (Δm), which is related to the frequency shift (Δf). For rigid and homogeneous films, there is a linear relationship between the surface concentration Γ_{QCM} and ($\Delta f/n$) according to the Sauerbrey equation for a given overtone (n):

$$\Gamma_{QCM} = -C\left(\frac{\Delta f}{n}\right)$$

where C is the mass sensitivity constant (17.7 ng·cm^{-2}·Hz^{-1}) for the crystals with a resonant frequency of 5 MHz. The linear relationship does not hold for flexible or soft films. The criterion for rigidity of the adsorbed layer used in this study is that $\Delta D/(\Delta f/n)$ is less than 1×10^{-7}.

Since the Δf represents the total surface mass change, including the mass of adsorbed proteins and coupled water, the water content of the adsorbed layer can be calculated by combining the information of Γ_{SPR} and Γ_{QCM}:

$$Water\ content = \left(\frac{\Gamma_{QCM} - \Gamma_{SPR}}{\Gamma_{QCM}}\right)\times 100\%$$

It should be noted that the calculated water content above is not a simple measure of the entrapped water in the adsorbed protein. The water-related mass change measured by QCM includes the mass increase due to the water molecules that are coupled with the adsorbed protein ($\Delta m_{\text{coupled}}$) and the mass decrease due to the exclusion of water at the protein–surface interface ($\Delta m_{\text{p-s}}$) as well as the interface between adjacent protein molecules ($\Delta m_{\text{p-p}}$). Thus, the total water-related mass change, Δm_{total}, can be expressed as

$$\Delta m_{total} = \Delta m_{coupled} - \Delta m_{p\text{-}s} - \Delta m_{p\text{-}p}$$

$\Delta m_{coupled}$ may depend on the conformation of the adsorbed protein. $\Delta m_{p\text{-}s}$ depends on the area occupied by the adsorbed protein and the thickness of the water layer on the surface. While the former is related to the conformation and orientation of the adsorbed protein (*e.g.* end on *versus* side on); the latter depends on the hydrophobicity of the surface. A hydrophobic surface has a thinner water layer than a hydrophilic one, resulting in a smaller mass decrease per unit area due to water displacement. Finally, $\Delta m_{p\text{-}p}$ depends on the proximity and packing of the protein molecules on the surface.

4.4 Results and discussion

4.4.1 Characterization of CA with different DS

CA is derived from cellulose by substituting the hydroxyl hydrogen atoms with acetyl groups. The chemical structure of CA is shown in Figure 4.1. The maximum attainable degree of substitution (DS) with acetyl groups per anhydroglucose unit is 3. The DS values for the three CA materials used in this study were calculated from the nominal acetyl contents and determined from ^{1}H NMR spectra (Appendix A). The calculated and measured DS values are compared in Table 4.1. The measured DS values, ranging from 1.9 to 3.0, are slightly higher than the calculated ones, ranging from 1.8 to 2.9. For reference, CA used for hemodialysis membranes has a DS of 2.5 (cellulose diacetate, *e.g.* Diaphan®) or 2.85 (cellulose triacetate). (It should be pointed out that the CAs used in this study likely contained trace amounts of lignin and hemicellulose because it was presumably derived from wood pulp, whereas CA used for commercial hemodialysis membranes is derived from cotton to avoid such contamination [11].) For

simplicity, to reflect their measured DS, CA-320, CA-398, and CA-436 are denoted henceforth CA18, CA25, and CA29, respectively.

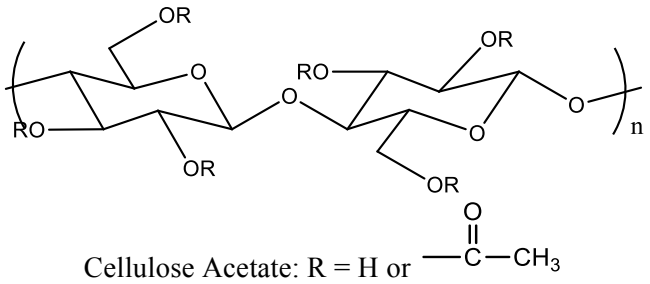

Figure 4.1 Molecular structure of CA

Table 4.1 Acetyl contents, DS values, and solubility parameters of CA materials

	Nominal acetyl content (wt%)	Calculated DS	Measured DS[a]	Solubility parameter ($MPa^{½}$)
CA 18	0.320	1.75	1.88	25.99
CA 25	0.398	2.45	2.61	23.30
CA 29	0.436	2.86	2.98	22.01

[a]By NMR spectroscopy

As a measure of hydrophobicity, the solubility parameters (SPs) of the CAs were estimated with the method proposed by Fedors [12]. This method calculates the SP, δ, by adding atomic and group contributions to the energy of vaporization and molar volume according to

$$\delta = \sqrt{\frac{\sum_i \Delta e_i}{\sum_i \Delta v_i}} = \sqrt{\frac{\Delta E_v}{V}}$$

where Δe_i is the group contribution to the energy of vaporization, Δv_i is the group contribution to the molar volume, ΔE_v is the energy of vaporization at a given temperature, and V is the corresponding molar volume. The group contributions at 25 °C were obtained from the same publication [12]. The SPs obtained for the three CAs, which are listed in Table 4.1, decrease with increasing DS, indicating an increase in hydrophobicity.

The surface morphologies of the three CA films, spincoated onto the gold-coated sensors, were investigated by AFM. Representative AFM height images for CA 18, CA 25, and CA 29 are shown in Figure 4.2. All films were homogeneous but CA 25 and CA 29 contained a few aggregates. The root mean square (RMS) roughness values calculated from 2 μm × 2 μm areas for CA 18, CA 25, CA 29 were 1.0 ± 0.2 nm, 2.2 ± 0.4 nm and 2.0 ± 0.3 nm, respectively.

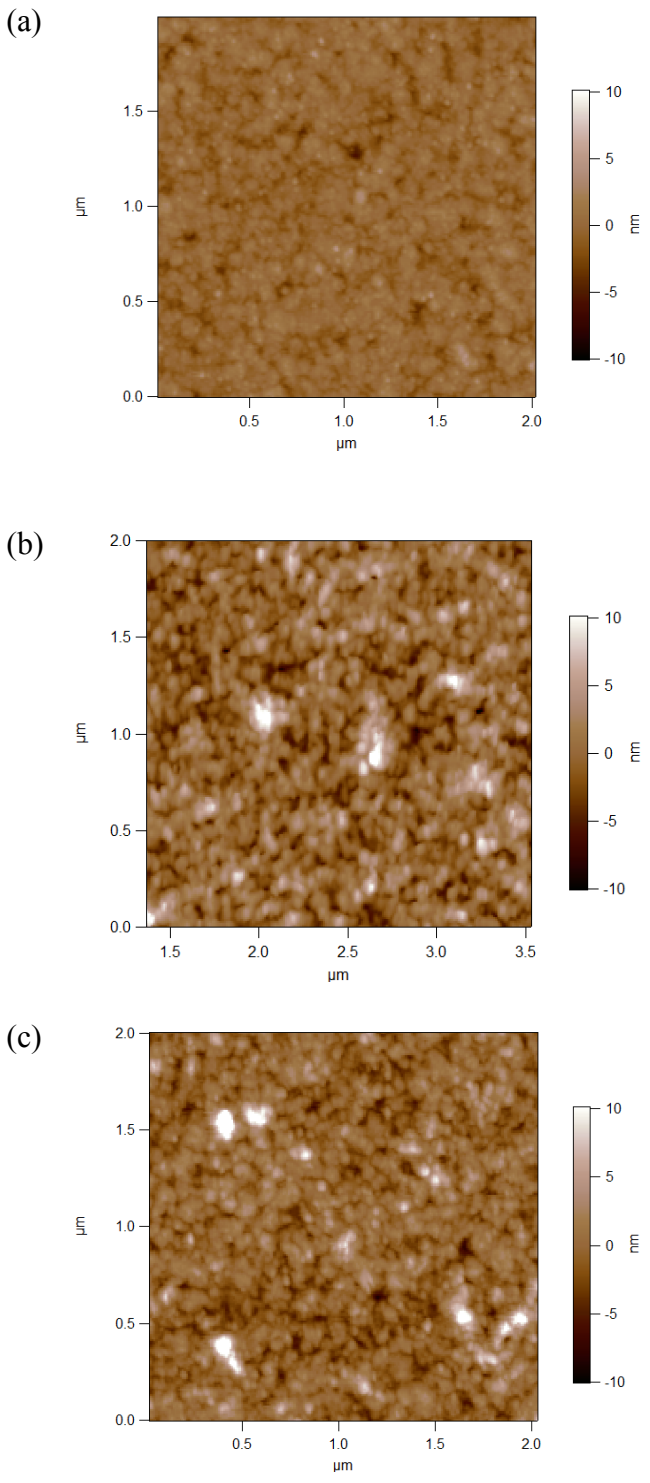

Figure 4.2 Representative of AFM height images of (a) CA 18, (b) CA 25, and (c) CA 29

4.4.2 Adsorption of HSA onto CA surfaces with different acetyl contents

Representative $\Delta\theta_{sp}$ and $(\Delta f/n)$ curves for HSA adsorption onto the three CA surfaces are shown in Figure 4.3 and Figure 4.4, respectively. The surface concentrations of irreversibly adsorbed HSA and water contents after buffer rinse are summarized in Table 4.2.

As seen in Figure 4.3, the $\Delta\theta_{sp}$ *versus* time curves for HSA adsorption onto the three CA surfaces are very similar. HSA adsorption onto CA29, the most hydrophobic of the CAs, was slightly faster than onto the other two CA surfaces. This finding is in agreement with the findings of Roach *et al.* who have studied the adsorption of bovine serum albumin onto CH_3 and OH-terminated self-assembled monolayers and observed more rapid adsorption onto the CH_3-terminated SAM [13]. The amount of irreversibly adsorbed HSA (Γ_{SPR}, Table 4.2) increased in the order: CA18, CA29, and CA25. Thus, rather than with DS, the amount of irreversibly adsorbed HSA might correlate with another factor, such as surface roughness or topology.

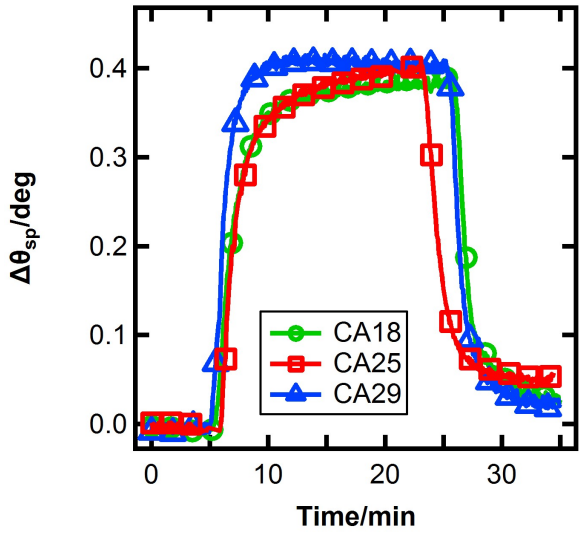

Figure 4.3 Representative SPR curves for HSA adsorption onto three CA surfaces differing in DS

With respect to the ($\Delta f/n$) *versus* time curves (Figure 4.4 A), while the curves for CA25 and CA29 were are similar, that for CA18 shows a much smaller frequency change upon HSA adsorption. The calculated water contents of the adsorbed layers on CA25 and CA29 are both fairly high (95 and 97%, respectively), whereas that of the adsorbed layer on CA 18 is lower (~75%). Surprisingly, the water content of the adsorbed layer does not correlate linearly with the DS values or hydrophobicity (SP values) of the CA surfaces. If the correlation were linear, the ($\Delta f/n$) values for HSA adsorption onto CA25 would lie between those for HSA adsorption onto CA18 and CA29. However, the ($\Delta f/n$) curve for CA25 was almost identical to that for CA29. There appeared to be a sudden change in water content of the HSA layer when the DS value of the CA surface exceeded a hydrophobicity threshold. Additional experiments with CAs of different DS are needed to explain this observation.

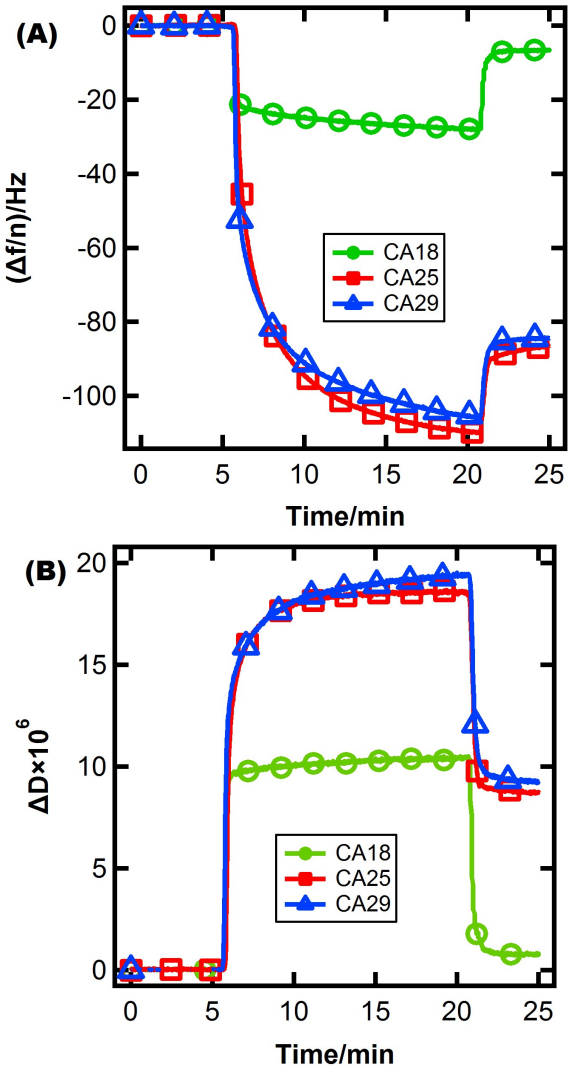

Figure 4.4 Representative QCM-D (A) frequency change and (B) dissipation change for HSA adsorption onto three CA surfaces (overtone n=5)

Table 4.2 Surface concentrations and water content of adsorbed HSA layers

	CA18	CA25	CA29
Γ_{SPR}(mg/m^2)	0.35 ± 0.03	0.83 ± 0.08	0.47 ± 0.07
$-\Delta D/(\Delta f/n)(\times 10^{-7})$	1.10 ± 0.03	1.00± 0.06	1.02 ± 0.06
Γ_{QCM}(mg/m^2)	1.45 ± 0.27	15.68 ± 0.68	14.28± 0.26
Water Content (%)	75.4 ± 5.0	94.7 ± 0.5	96.7 ± 0.5

As discussed in Section 4.3.5, the water-related mass change measured by QCM is a net result of mass changes caused by protein adsorption. A larger Δm_{total} on one CA surface with respect to another could be caused by a smaller $\Delta m_{p\text{-}p}$ (lower packing density), a smaller $\Delta m_{p\text{-}s}$ (smaller binding area or higher surface hydrophobicity), and a larger $\Delta m_{coupled}$ (related to the protein conformation). Assuming a globular shape and a diameter of 7 nm for HSA [14, 15], the HSA surface concentration at full surface coverage is about 2.3 mg/m^2. The low measured surface concentrations relative to the theoretical saturation surface concentration might indicate that the protein molecules are not tightly packed. Thus, the contribution of $\Delta m_{p\text{-}p}$ to Δm_{total} is likely small. The lower water exclusion (smaller $\Delta m_{p\text{-}s}$) on more hydrophobic surfaces could be one reason for the larger measured water contents (Δm_{total} values) of the HSA layers on CA25 and CA29. Another possible explanation is the conformation of adsorbed HSA molecules, which affects $\Delta m_{coupled}$ as well as $\Delta m_{p\text{-}s}$ through the protein binding area, may be different on CA18 and the more hydrophobic CA surfaces. Different HSA conformations could

also be the reason for the slightly higher flexibility (–ΔD/(Δf /n)) of the adsorbed HSA layer on CA18 compared to those on CA25 and CA29.

Sivaraman *et al.* have shown that at a solution concentration of 1.0 mg/mL, the conformation of HSA adsorbed onto OH-terminated SAM surfaces differs significantly from that of HSA adsorbed onto CH_3-terminated SAM surfaces [12]. Specifically, HSA on CH_3-terminated SAM surfaces has equal contents of α-helix and β-sheet in its secondary structure whereas HSA on OH-terminated SAM surface has much more α-helix than β-sheet, more closely resembling the conformation of HSA in solution. Thus, the secondary structure of HSA adsorbed onto CA18 could be different from that of HSA adsorbed onto CA25 or CA29. However, since the acetyl content increases gradually from CA18 to CA29, one would expect a gradual increase in water content if the number of HSA molecules in the predominantly α-helix conformation was proportional to the number of hydroxyl groups present. Also, it has been shown that conformational changes of HSA are much less pronounced at higher solution concentration (10 mg/mL) [3] with minimal degree of adsorption-induced unfolding expected at plasma concentrations (40 mg/mL).

At this point, it is worth mentioning that the first batch of HSA used in our experiments exhibited a markedly different adsorption behavior on CA25 than the subsequent batches. The ($\Delta f/n$) curve initially resembled that for HSA adsorption onto CA29 until a frequency change of –50 Hz was reached at which point it exhibited a sudden increase in ($\Delta f/n$) (Figure 4.5). In previous protein adsorption studies, such overshooting phenomena have been attributed to changes in protein orientation or desorption after initial adsorption [16]. Here, the overshooting phenomenon would be

consistent with a change in HSA conformation on the CA25 surface from an initially highly hydrated one, similar to that observed on CA29, to a water-excluding secondary structure similar to that observed on CA18.

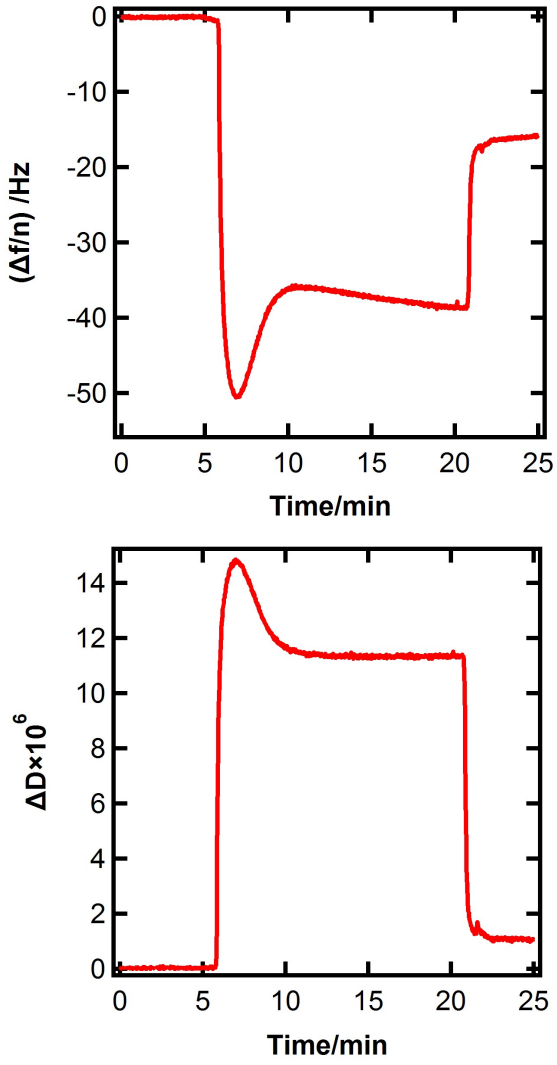

Figure 4.5 Representative QCM-D (left) frequency change and (right) dissipation change for first batch HSA adsorption onto CA25 (overtone n = 5)

4.5 Conclusions

The relationship between the density of acetyl groups on CA surfaces and adsorption behavior of HSA has been explored by SPR and QCM-D. The adsorbed amount and water content of HSA layers on the CA surfaces have been calculated. A strong relationship between the adsorbed amount and the DS values of CA has not been found. Other factors, such as surface roughness and topology, may affect the adsorbed amount. There is a big difference in the water content of HSA layers. HSA adsorbed on CA with a low DS value is less hydrated than that on CA with a high DS value. The difference in water content may indicate differences in HSA conformation on the different CA surfaces or could be an artifact of the analytical technique resulting from a difference in surface hydrophobicity. More strong and direct evidence for conformational differences of the adsorbed protein is needed to test this hypothesis.

4.6 Acknowledgements

This material is based upon work supported in part by the National Science Foundation under grant number DMR-0907567. Moreover, this work was supported in part by the Virginia Agricultural Experiment Station and the USDA National Institute of Food and Agriculture, Hatch/Multi State project 1002269 and grant number 2010-65504-20429. Partial funding from the Macromolecules and Interfaces Institute is also acknowledged.

4.7 References

[1] Schaller, J. Human blood plasma proteins : structure and function. John Wiley & Sons: Chichester, West Sussex, England; Hoboken, NJ, 2008.

[2] Vroman, L. When Blood Is Touched. Materials 2009, 2, 1547-1557.

[3] Sivaraman, B.; Latour, R. A. Time-dependent conformational changes in adsorbed albumin and its effect on platelet adhesion. Langmuir 2012, 28, 2745-52.

[4] Liu, X.; Yuan, L.; Li, D.; Tang, Z.; Wang, Y.; Chen, G.; Chen, H.; Brash, J. L. Blood compatible materials: state of the art. Journal of Materials Chemistry B 2014, 2, 5718-5738.

[5] Daugirdas, J. T.; Bernardo, A. A. Hemodialysis effect on platelet count and function and hemodialysis-associated thrombocytopenia. Kidney Int 2012, 82, 147-157.

[6] De Feijter, J. A.; Benjamins, J.; Veer, F. A. Ellipsometry as a tool to study the adsorption behavior of synthetic and biopolymers at the air–water interface. Biopolymers 1978, 17, 1759-1772.

[7] Malmsten, M. Ellipsometry Studies of Protein Adsorption at Lipid Surfaces. J Colloid Interface Sci 1994, 168, 247-254.

[8] Kittle, J. D.; Du, X.; Jiang, F.; Qian, C.; Heinze, T.; Roman, M.; Esker, A. R. Equilibrium Water Contents of Cellulose Films Determined via Solvent Exchange and Quartz Crystal Microbalance with Dissipation Monitoring. Biomacromolecules 2011, 12, 2881-2887.

[9] Kaya, A.; Du, X.; Liu, Z.; Lu, J. W.; Morris, J. R.; Glasser, W. G.; Heinze, T.; Esker, A. R. Surface Plasmon Resonance Studies of Pullulan and Pullulan Cinnamate Adsorption onto Cellulose. Biomacromolecules 2009, 10, 2451-2459.

[10] http://www.matbase.com/material-categories/natural-and-synthetic-polymers/thermoplastics/engineering-polymers/material-properties-of-synthetic-cellulose-acetate-ca.html - properties

[11] Bouré, T.; Vanholder, R. Which dialyser membrane to choose? Nephrology Dialysis Transplantation 2004, 19, 293-296.

[12] Fedors, R. F. A method for estimating both the solubility parameters and molar volumes of liquids. Polymer Engineering & Science 1974, 14, 147-154.

[13] Roach, P.; Farrar, D.; Perry, C. C. Interpretation of Protein Adsorption: Surface-Induced Conformational Changes. Journal of the American Chemical Society 2005, 127, 8168-8173.

[14] Kiselev, M. A.; Gryzunov Iu, A.; Dobretsov, G. E.; Komarova, M. N. Size of a human serum albumin molecule in solution. Biofizika 2001, 46, 423-7.

[15] Ferrer, M. L.; Duchowicz, R.; Carrasco, B.; de la Torre, J. G.; Acuna, A. U. The conformation of serum albumin in solution: a combined phosphorescence depolarization-hydrodynamic modeling study. Biophys J 2001, 80, 2422-30.

[16] Rabe, M.; Verdes, D.; Seeger, S. Understanding protein adsorption phenomena at solid surfaces. Advances in Colloid and Interface Science 2011, 162, 87-106.

Chapter 5 Overall conclusions and suggestions for future work

5.1 Overall conclusions

In this study, surface plasmon resonance and quartz crystal microbalance with dissipation monitoring have been combined to investigate the adsorption behavior of two platelet adhesion-related blood proteins, human serum albumin (HSA) and human serum fibrinogen (HSF), on two polysaccharide materials used in hemodialysis membrane applications: regenerated cellulose (RC) and cellulose acetate (CA). The study aims to provide new insights for the design of novel hemocompatible polysaccharide materials. Information, such as the real-time adsorption curve, the adsorbed amount, and the water content of the protein layers, were obtained for different protein–polysaccharide combinations. It was found that 1) irreversible HSA adsorption was greater on CA than on RC surfaces; 2) on both surfaces, the mass of adsorbed HSA was much smaller than expected for a densely packed monolayer; 3) on CA surfaces, irreversibly adsorbed HSA had a greater water content than on RC surfaces; 4) irreversible HSF adsorption reached similar masses on both surfaces; 5) the adsorbed mass of HSF equaled or slightly exceeded that expected for a densely packed side-on monolayer, suggesting some degree of end-on or multiple layer adsorption, 6) irreversibly adsorbed HSF on RC surfaces has a low water content; and 7) on CA surfaces, gradual HSF desorption of the protein layer occurred.

Further study of the adsorption of HSA on three CA surfaces with different degrees of substitution (DS) was also conducted. The adsorbed amount was correlated with surface roughness. Irreversibly adsorbed HSA on CA of low DS (≈ 1.8) excluded water whereas that on CA of higher DS (≥ 2.5) had a high water content (≥ 95%). The difference in water contents of

adsorbed HSA on CA of low and higher DS might suggest different protein conformations on these surfaces.

5.2 Suggestions for future work

Because our attempts to determine the conformations of the adsorbed proteins on the RC and CA surfaces by Raman and circular dichroism spectroscopy were unsuccessful, all explanations for the different water contents are based on a combination of considerations from our experimental results, previous knowledge from the literature, and speculation. Additional experiments such as atomic force microscopy, circular dichroism spectroscopy, and infrared spectroscopy are needed for confirmation. The main challenge is the characterization of the proteins adsorbed on the surface made difficult by the low sensitivity of analytical methods relative to the mass of surface adsorbed protein.

Polysaccharides are a broad class of materials with similar chemical composition and functional groups that can be modified selectively. Other polysaccharide materials used for topical hemostatic agents such as oxidized cellulose, chitin, and chitosan also come in contact with blood. Similar studies of the interactions between blood proteins and material surfaces could be done with these materials to provide a deeper insight.

Future work could also include different proteins. Blood coagulation is a very complicated process that involves interactions of more than one protein under in vivo conditions. The main challenges in this area include that the exact mechanisms of how protein–surface interactions affect responses such as blood coagulation and complement activation and, thus, the hemocompatibility of materials are incompletely understood.

Appendix A

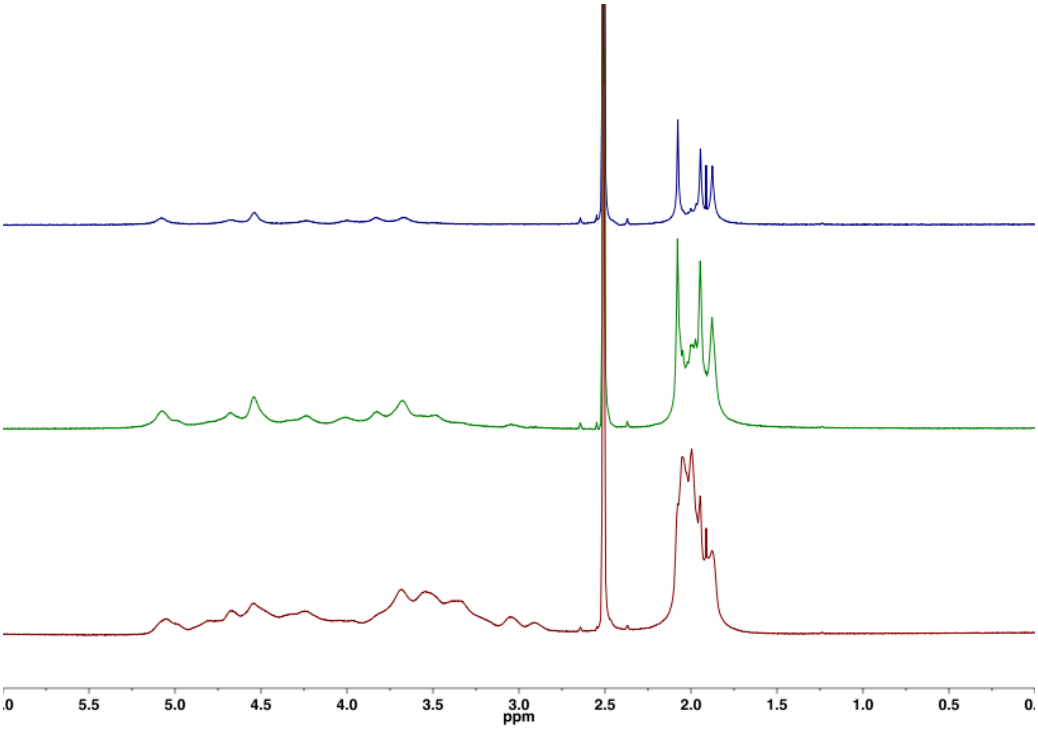

Figure A. 1 NMR spectrum for the three CA materials: CA29 (top), CA25 (middle) and CA18 (bottom)

The DS values of the cellulose acetates are obtained by calculating the ratio of the acetyl proton integrals (A_{acetyl}) to that of the backbone protons (A_{backbone}). The acetyl protons are between 1.88 and 2.25 ppm, and the backbone protons are between 5.25 to 2.75 ppm.

$$\frac{A_{\text{acetyl}}}{A_{\text{backbone}}} = \frac{3\times\text{DS}}{7}$$

$$\text{DS} = \frac{7}{3} \times \frac{A_{\text{acetyl}}}{A_{\text{backbone}}}$$